

A Nonlinear African Vulture Optimization Algorithm Combining Henon Chaotic Mapping Theory and Reverse Learning Competition Strategy

Baiyi Wang¹, Zipeng Zhang¹, Patrick Siarry², Xinhua Liu¹, Grzegorz Królczyk³, Dezheng Hua¹,

Frantisek Brumercik⁴, Zhixiong Li^{5*}

1. School of Mechatronic Engineering, China University of Mining and Technology, Xuzhou, China

2. University Paris-Est Créteil Val de Marne, 61 Av. du General de Gaulle, 94010, Creteil, France

3. Department of Manufacturing Engineering and Automation Products, Opole University of Technology, 45-758 Opole, Poland

4. Department of Design and Machine Elements, Faculty of Mechanical Engineering, University of Zilina, Univerzitna 1, 010 26 Zilina, Slovakia

5. Yonsei Frontier Lab, Yonsei University, Seoul 03722, South Korea

Emails: ts22050054a311d@cumt.edu.cn (Baiyi Wang); cnzpz@cumt.edu.cn (Zipeng Zhang); siarry@u-pec.fr (Patrick Siarry); liuxinhua@cumt.edu.cn (Xinhua Liu); g.krolczyk@po.edu.pl (Grzegorz Królczyk); hua_dezheng@cumt.edu.cn (Dezheng Hua); frantisek.brumercik@fstroj.uniza.sk (Frantisek Brumercik)

* Corresponding author: zhixiong.li@yonsei.ac.kr (Zhixiong Li)

Abstract: As a new intelligent optimization algorithm, the African vultures optimization algorithm (AVOA) has been widely used in various fields today. However, when solving complex multimodal problems, the AVOA still has some shortcomings, such as low searching accuracy, deficiency on the search capability and tendency to fall into local optimum. In order to alleviate the main shortcomings of the AVOA, a nonlinear African vulture optimization algorithm combining Henon chaotic mapping theory and reverse learning competition strategy (HWEAVOA) is proposed. Firstly, the Henon chaotic mapping theory and elite population strategy are proposed to improve the randomness and diversity of the vulture's initial population; Furthermore, the nonlinear adaptive incremental inertial weight factor is introduced in the location update phase to rationally balance the exploration and exploitation abilities, and avoid individual falling into a local optimum; The reverse learning competition strategy is designed to expand the discovery fields for the optimal solution and strengthen the ability to jump out of the local optimal solution. HWEAVOA and other advanced comparison algorithms are used to solve classical and CEC2022 test functions. Compared with other algorithms, the convergence curves of the HWEAVOA drop faster and the line bodies are smoother. These experimental results show the proposed HWEAVOA is ranked first in all test functions, which is

superior to the comparison algorithms in convergence speed, optimization ability, and solution stability. Meanwhile, HWEAVOA has reached the general level in the algorithm complexity, and its overall performance is competitive in the swarm intelligence algorithms.

Keywords: African vultures optimization algorithm; Henon chaotic mapping theory; Nonlinear adaptive incremental inertial weight factor; Reverse learning competition strategy.

1. Introduction

Optimization problems are common in many fields, such as intelligent production, scientific research, and economic management. Today, the complexity and difficulty of optimizing issues are increasing, and solutions are becoming more dynamic and computationally complex. Finding one or more points in a multidimensional hyperspace is often necessary. Traditional data processing methods are increasingly difficult to cope with the data surge problems brought at the digital age. Therefore, intelligent optimization algorithms are needed to determine an accurate solution for us (Kar, 2016; D. Karaboga & Akay, 2009; Li, Wang, & Gandomi, 2021). The intelligent optimization algorithm is a new optimization algorithm that simulates biological behaviours and some natural physical phenomena. With the appliance of these algorithms, many complex optimization problems can be solved efficiently (Valdez, Castillo, Cortes-antonio, & Melin, 2022). Compared with a traditional optimization algorithm, an intelligent optimization algorithm converges fast, robust, pervasive and stable (Cui, Geng, Zhu, & Han, 2017; Nabaei, et al., 2018). In recent years, intelligent optimization algorithms have developed unprecedently. Scholars put forward a series of new intelligent optimization algorithms, such as the supply-demand-based optimization (Zhao, Wang, & Zhang, 2019), carnivorous plant algorithm (Meng, Pauline, & Kiong, 2021), honey badger optimization algorithm (Hashim, Houssein, Hussain, Mabrouk, & Al-Atabany, 2022), Runge Kutta optimization algorithm (Ahmadianfar, Heidari, Gandomi, Chu, & Chen, 2021), hunger game search algorithm (Yang, Chen, Heidari, & Gandomi, 2021), wild horse optimization algorithm (Naruei & Keynia, 2022), material generation optimization algorithm (Oyelade, Ezugwu, Mohamed, & Abualigah, 2022), spider jumping optimization algorithm (Peraza-Vazquez, et al., 2022), reptile search algorithm (Abualigah, Abd Elaziz, Sumari, Geem, & Gandomi, 2022), capuchin search algorithm (Braik, Sheta,

& Al-Hiary, 2021). The intelligent optimization is widely used in system identification (N. Karaboga, 2009), path planning (Wang, Yan, & Gu, 2019), troubleshooting (Deng, Li, Li, Chen, & Zhao, 2022), neural networks (Xu, Yu, & Gulliver, 2021), optimization control (Hamza, Yap, & Choudhury, 2017) and other fields (Kalinli & Karaboga, 2005; N. Karaboga & Cetinkaya, 2011) for good searchability.

The African vultures optimization algorithm (AVOA) (Abdollahzadeh, Gharehchopogh, & Mirjalili, 2021) is a new intelligent optimization algorithm proposed by Benyamin Abdollahzadeh et al. in 2021, which simulates the foraging and navigation behaviours of African vultures. The algorithm has the advantages of simple structure, easy implementation and outstanding performance in finding optimal values, which has been well applied in various fields. (Salah, et al., 2022) introduced the African vultures optimization algorithm to optimize the PID controller and apply it to control DC microgrid voltage. (Mekala, Sumathi, & Shobana, 2022) proposed a multi-polymer charging scheduling strategy based on AVOA to realize the proper planning of electric vehicle charging. (Singh, Houssein, Mirjalili, Cao, & Selvachandran, 2022) introduced the African vulture algorithm to optimize solutions to the travel salesman shortest path problem. (Diab, Tolba, El-Rifaie, & Denis, 2022) introduced the African vulture algorithm to accurately predict unknown parameters of various solar photovoltaic units. (Zhang, Khayatnezhad, & Ghadimi, 2022) applied the African vulture algorithm to the actual PEMFC baseline case study and established an optimal evaluation model for fuel cells.

Although the AVOA has a large amount of applications, it still shows deficiency on the search capability and tendency to fall into local optimum. To solve these problems of the AVOA, (Liu, et al., 2022) introduced quasi-antagonistic learning mechanisms, differential evolution operators and adaptive parameters to balance AVOA exploration and development capabilities. (Fan, Li, & Wang, 2021) uses chaotic mapping and time-varying tool to optimize the global optimal solution and convergence performance of AVOA. (Soliman, Hasanien, Turkey, & Muyeen, 2022) proposed a new African vulture-grey wolf hybrid optimizer to improve the convergence speed and stability of the algorithm. (Kannan, Mannathazhathu, & Raghavan, 2022) proposed a hybrid optimization algorithm based on honey badger and African vulture, the global optimization search of the algorithm is implemented, and the probability of falling into the local optimum is reduced.

To date, due to the novelty, there are few studies on the improvements of AVOA. Although the existing improved AVOA increases the optimization performance, there are still some limitations and uncertainties, such as the lack of diversity in initialized populations, the unbalance of the exploration and exploitation capabilities, and the waste of valuable population information, which resulting in the AVOA algorithm is sensitive to local optimal, cannot get the ideal solution. Therefore, an improved AVOA with multi-strategy (HWEAVOA) is proposed to eliminate the uncertainty and restriction of the original AVOA, and subsequently improve its algorithm's performance. Firstly, Henon chaotic mapping theory and elite population strategy (HCE) are proposed, which make the initial population distribution more homogeneous, enhance the global optimization performance and the convergence rate of the AVOA. Then, the nonlinear adaptive incremental inertial weight factor (NWF) is introduced to optimally update the position of vultures. This strategy can assist vulture populations to search at different convergence rates, which balances the exploration and exploitation abilities, and effectively avoids AVOA falling into a local optimum. Finally, the reverse learning competition strategy (RLC) is designed to increase the diversity of the population. The bad performed vulture individuals are given learning opportunities, and they will have the probability to become dominant individuals. This strategy expands the discovery fields for the optimal solution and avoids the generation of local optimum phenomenon.

To evaluate the effectiveness of the HWEAVOA algorithm, classical and CEC2022 test functions are used to compare the optimization performance of the AVOA and other improved algorithms.

The rest of this paper is organized as follows. In Section 2, the original AVOA is briefly introduced. In section 3, the technical details of the HWEAVOA algorithm are described. In section 4, the performance of HWEAVOA is analyzed reliably by using classical and CEC2022 test functions. In section 5, this study is summarized by discussing the results and possible future areas for potential investigations are puts forward.

2. African vultures optimization algorithm (AVOA)

The African vultures optimization algorithm (AVOA) simulates the foraging and navigation behaviours of African vultures from the African vulture lifestyle. Each individual in the population relies on their hunger rate for corresponding behaviours and completes the switch between the

exploration and development stages. The hunger rate is calculated as follows:

$$M = h \times \left(\sin^W \left(\frac{\pi}{2} \times \frac{t}{T} \right) + \cos \left(\frac{\pi}{2} \times \frac{t}{T} \right) - 1 \right) \quad (1)$$

$$F = (2 \times rand_1 + 1) \times z \times \left(1 - \frac{t}{T} \right) + M \quad (2)$$

Where: F is the vulture hunger rate, t indicates the current number of iterations, T is the maximum number of iterations, W shows a fixed parameter set before the algorithm works, z represents a random number between -1 and 1, h represents a random number between -2 and 2, and $rand_1$ indicates a random number between 0 and 1.

When the F value is greater than 1, the vulture searches for food in different regions and enters the exploration phase, using formula (3) to search for food in other areas.

$$P(i+1) = \begin{cases} \text{Optimal solution guidance strategy, if } P_1 \geq rand_{p_1} \\ \text{Random search strategy, if } P_1 < rand_{p_1} \end{cases} \quad (3)$$

Where: P_1 is a control parameter with values between 0 and 1; $rand_{p_1}$ represents a random number between 0 and 1.

About the optimal solution guidance strategy, the remaining vultures search for food near one of the optimal vultures at a random distance. The position update formula is as follows:

$$P(i+1) = R(i) - |X \times R(i) - P(i)| \times F \quad (4)$$

Where: $P(i+1)$ represents the vulture position vector in the next iteration, F is the hunger rate of vulture individuals in the current iteration. X is a place where vultures move randomly, which is used as a coefficient vector to increase random motion and obtained by using the formula $X = 2rand$, where $rand$ is a random number between 0 and 1; $P(i)$ indicates the current vector position of the vulture. $R(i)$ indicates the best vulture chosen at random, and the solution formula is as follows:

$$R(i) = \begin{cases} BestV_1, p_i = L_1 \\ BestV_2, p_i = L_2 \end{cases} \quad (5)$$

Where $BestV_1$, $BestV_2$ represents the two best adapted vultures in the vulture population

respectively; L_1, L_2 represents the parameters between $0 \sim 1$ which waited to be measured respectively, and their sum is 1; p_i represents the probability of selecting the best vulture;

On the other hand, vultures perform random search strategies with the following positional update formula (6).

$$P(i+1) = R(i) - F + rand_2 \times ((ub - lb) \times rand_3 + lb) \quad (6)$$

Where $rand_2$ and $rand_3$ are random values between 0 and 1, lb and ub represent the upper and lower bounds of the variable.

If the value of F is less than 1, the vulture enters the development phase and looks for food near the best solution. When $0.5 \leq |F| \leq 1$, as shown in Fig. 1, the population gets food through the implementation of the conflict profit strategy and rotational flight strategy, the two methods are selected and executed by formula (7).

$$P(i+1) = \begin{cases} \text{Conflict profit strategy, if } P_2 \geq rand_{P_2} \\ \text{Rotational flight strategy, if } P_2 < rand_{P_2} \end{cases} \quad (7)$$

where P_2 is a control parameter with values between 0 and 1; $rand_{P_2}$ is a random number between 0 and 1.

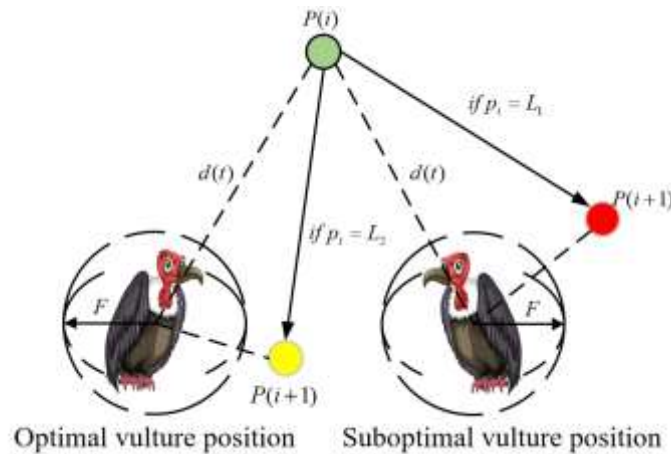


Fig. 1. The schematic map of vulture populations vying for food.

About the conflict profitability strategy, weak vultures try to get food by causing conflicts between healthy vultures to fatigue them, and their position update formula is updated as follows:

$$P(i+1) = |X \times R(i) - P(i)| \times (F + rand_4) - (R(i) - P(i)) \quad (8)$$

where $rand_4$ is a random number between 0 and 1.

In addition, the vulture rotational flight strategy is as follows:

$$\begin{cases} S_1 = R(i) \times \left(\frac{rand_5 \times P(i)}{2\pi} \right) \times \cos(P(i)) \\ S_2 = R(i) \times \left(\frac{rand_6 \times P(i)}{2\pi} \right) \times \sin(P(i)) \end{cases} \quad (9)$$

$$P(i+1) = R(i) - (S_1 + S_2) \quad (10)$$

where $rand_5$ and $rand_6$ are random numbers between 0 and 1; S_1 and S_2 are calculated by formula (8). Finally, the vulture position update is completed by formula (9).

When $|F| \leq 0.5$, as shown in Fig. 2, the population gets food through the implementation of individual competition strategy and population competition strategy, two methods are selected and executed by formula (11).

$$P(i+1) = \begin{cases} \text{Individual competition strategy, if } P_3 \geq rand_{p_3} \\ \text{Population competition strategy, if } P_3 < rand_{p_3} \end{cases} \quad (11)$$

where P_3 is a control parameter with values between 0 and 1; $rand_{p_3}$ is a random number between 0 and 1.

When an individual competition strategy is implemented, multiple vultures may accumulate on the same food source, and the position update formula is as follows:

$$\begin{cases} A_1 = BestV_1 - \frac{BestV_1 \times P(i)}{BestV_1 - P(i)^2} \times F \\ A_2 = BestV_2 - \frac{BestV_2 \times P(i)}{BestV_2 - P(i)^2} \times F \end{cases} \quad (12)$$

$$P(i+1) = \frac{A_1 + A_2}{2} \quad (13)$$

When a population competition strategy is implemented, multiple vultures may accumulate on the same food source, and the position update formula is as follows:

$$P(i+1) = R(i) - |R(i) - P(i)| \times F \times Levy \quad (14)$$

where $Levy$ indicates the levy flight.

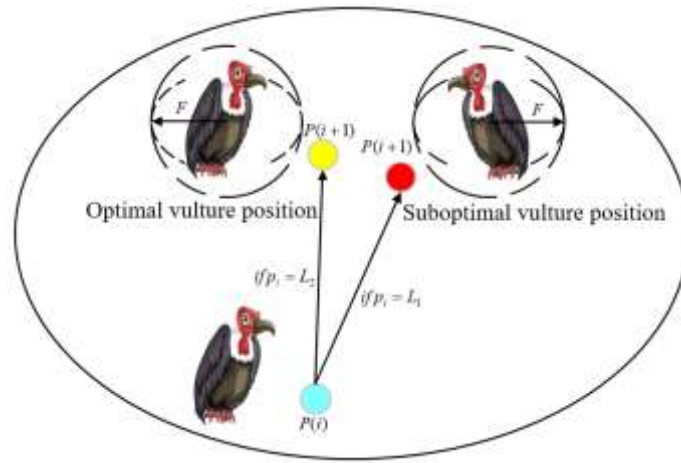


Fig. 2. The schematic map of vulture individuals fiercely competing for food.

3. The proposed optimization algorithm (HWEAVOA)

As mentioned above, although the overall mechanism of the AVOA algorithm is simple and easy to implement, it still has some limitations, such as the lack of diversity in initialized populations, the unbalance of the exploration and exploitation capabilities, and the waste of valuable population information, which resulting in the AVOA algorithm is sensitive to local optimal, cannot get the ideal solution. In this section, three improvement strategies are proposed, namely the Henon chaotic mapping theory and elite population strategy (HCE), the nonlinear adaptive incremental inertial weight factor (NWF), and the reverse learning competition strategy (RLC), which will be discussed in the following sections.

3.1 Henon chaotic mapping theory and elite population strategy (HCE)

The primitive vulture population is initialized by randomization, with an uneven distribution and lacking population. Cause of low randomness, primitive AVOA always faces high uncertainty. Therefore, if the homogeneous initialization of the population can be solved, the population diversity can be increased effectively, and the searching efficiency of the algorithm can be improved. To this end, Henon chaotic mapping theory and elite population strategy are introduced in this paper.

Henon chaotic mapping theory is a nonlinear theory with the characteristics of nonlinear, initial sensitivity, randomness and ergodicity. Henon chaotic map is produced in 2-dimensional space, a typical discrete chaotic map. Its kinetic formula is as follows:

$$\begin{cases} x_{n+1} = 1 + y_n - ax_n^2 \\ y_{n+1} = bx_n \end{cases} \quad (15)$$

Where the state of the Henon chaotic map is determined by the four parameters x_0 , y_0 , a , and b , which is more complex than the 1-dimensional chaotic map. This paper takes $a = 1.4$, $b = 0.3$ to ensure the strong randomness of the generated chaotic sequence when the function enters the chaotic state. By the above mapping method, the chaotic mapping initialization population is obtained.

Then, the elite population strategy is adopted by this paper, which combines the chaotic mapped initialized population and the conventional initialized population, calculates the adaptability of each initial vulture, and sorts it. At last, the first N elite individuals are selected, and the sequence of privileged individuals is as follows:

$$x_i = \{x_1, x_2, \dots, x_N\}, i = 1 \square N \quad (16)$$

Where $x_1 = BestV_1$, $x_2 = BestV_2$. N is the number of vultures in the population.

The above improved ways make the initial population distribution more homogeneous and give the initial population more possibilities, which enhances the global optimization performance and convergence rate of the AVOA.

3.2 Nonlinear adaptive incremental inertial weight factor (NWF)

In AVOA, the entire vulture population starts from the global search and gradually returns to local search, which performs mechanically the exploration phase and exploitation phase under the leadership of the optimal vulture and the suboptimal vulture. However, the whole process of algorithm is not static. It is difficult to effectively balance the global search stage and the local search stage of the population by using the original position update formula of AVOA. The entire process ignores the actual environment of the vulture population, which cause the AVOA is sluggish in convergence and prone to the local optimum. Therefore, the nonlinear adaptive incremental inertial weight factor is introduced to realize the rational allocation of the global exploration phase and local exploitation phase in different evolutionary periods in this paper.

The nonlinear adaptive incremental inertial weight factor ω is added to the process of the position renewal of vulture populations, which is calculated as follows:

$$\omega = \begin{cases} (\alpha + \beta \times rand) \times \sin\left(\frac{\pi}{10} \times \frac{t}{T}\right)^5, & \text{mod}\left(\frac{t}{6}\right) \geq 3 \\ 1 & , \text{mod}\left(\frac{t}{6}\right) \leq 3 \end{cases} \quad (17)$$

where α and β are the selection factors for the initial optimal vulture and the secondary vulture, and $rand$ is the random number of $0 \sim 1$. $\text{mod}\left(\frac{t}{6}\right)$ is the residual number of iterations divided by 6.

The nonlinear adaptive incremental inertial weight factor ω is then introduced into the vulture position update formulas in the exploration and development phases; the process is shown in formulas (18), (19) and (20).

$$P(i+1) = \begin{cases} \omega \times \text{Equation}(4) & \text{if } P_1 \geq rand_{P_1} \\ \omega \times \text{Equation}(6) & \text{if } P_1 < rand_{P_1} \end{cases} \quad (18)$$

$$P(i+1) = \begin{cases} \omega \times \text{Equation}(8) & \text{if } P_2 \geq rand_{P_2} \\ \omega \times \text{Equation}(10) & \text{if } P_2 < rand_{P_2} \end{cases} \quad (19)$$

$$P(i+1) = \begin{cases} \omega \times \text{Equation}(13) & \text{if } P_3 \geq rand_{P_3} \\ \omega \times \text{Equation}(14) & \text{if } P_3 < rand_{P_3} \end{cases} \quad (20)$$

The position of vultures is optimally updated through the above formula. This step considers evolutionary differences between population vultures during evolution, which adaptively confers inertial weight factors of different sizes. When the inertial weight factor ω increases, the global optimization ability of the algorithm is significantly enhanced. However, the local search ability is reduced, and the solution accuracy could be lower. When the inertial weight factor ω declines, the global optimization ability is decreased, while the local optimization ability is enhanced and the solution accuracy is higher. **The inertial weight factor assists vultures in searching at different convergence rates until they approach the optimal value in the next iteration. The inertial weight factor improves the search ability of the vulture population at different stages on the premise that the overall search behavior is unchanged. In the early stage of the population with a strong global search ability, its local search ability is improved appropriately, which increasing the search accuracy and convergence rate of the AVOA. In the later stage of the population with a strong local search ability, its global search ability is improved appropriately, which effectively avoiding AVOA falling into a**

local optimum. These characteristics meet the needs of the AVOA for global exploration ability and local exploitation ability at different evolutionary times.

3.3 Reverse learning competition strategy (RLC)

The information from the optimal location in the iteration process is used simply in the original AVOA, and part of the valuable information in the population is wasted easily. Therefore, the reverse learning competition strategy is introduced in this paper. **The main idea of reverse competitive learning strategy is to increase the diversity of the population and chance of obtaining better solutions by simultaneously exploring the positive and negative direction of search space simultaneously. As shown in Fig. 3, the bad performed vulture individuals are given more learning opportunities, and they will have the probability to become dominant individuals.** In this way, the loss of useful information is solved well and the accuracy of the next input is effectively guaranteed.

Based on each output solution, the reverse learning solution $E_p(i+1)$ is obtained through the reverse learning competition strategy. The calculation formula is as follows:

$$E_p(i+1) = rand \times (ub + lb) - P(i+1) \quad (21)$$

where $rand$ is a random number of $0 \sim 1$.

The output position of vultures in this iteration is optimized by calculating the population fitness of $P(i+1)$, and $E_p(i+1)$. In this way, the optimal individual position is not lost, and the optimal individual information can be used to significantly improve the robustness of AVOA algorithm.

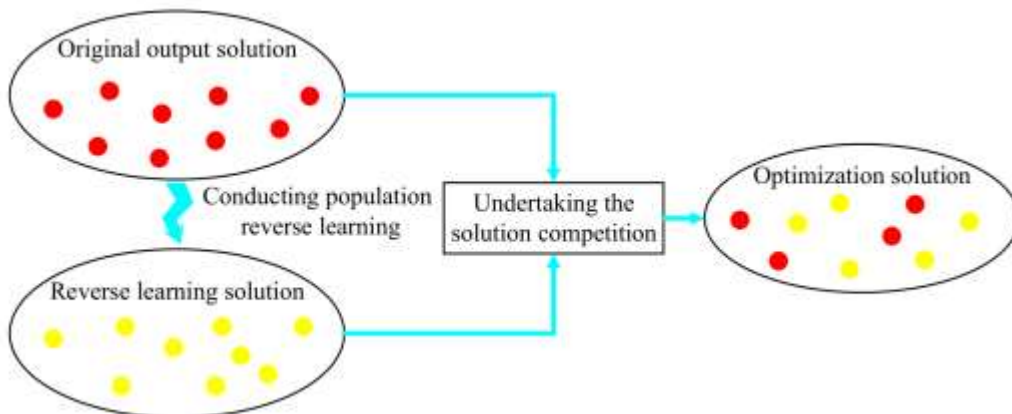


Fig. 3 Schematic map of reverse learning competition strategy.

In summary, the problems in the original AVOA algorithm, such as uneven population initialization individual distribution, lack of population diversity, no reasonable balance between

global and local search stages, and easy loss of better personal information, are well solved based on three strategies, i.e., HCE, NWF, and RLC, corresponding to the Henon chaotic mapping theory and elite population strategy, the nonlinear adaptive incremental inertial weight factor, the reverse learning competition strategy, respectively. The framework of HWEAVOA algorithm is shown in the Fig. 4 and its technical details are described in Table 1.

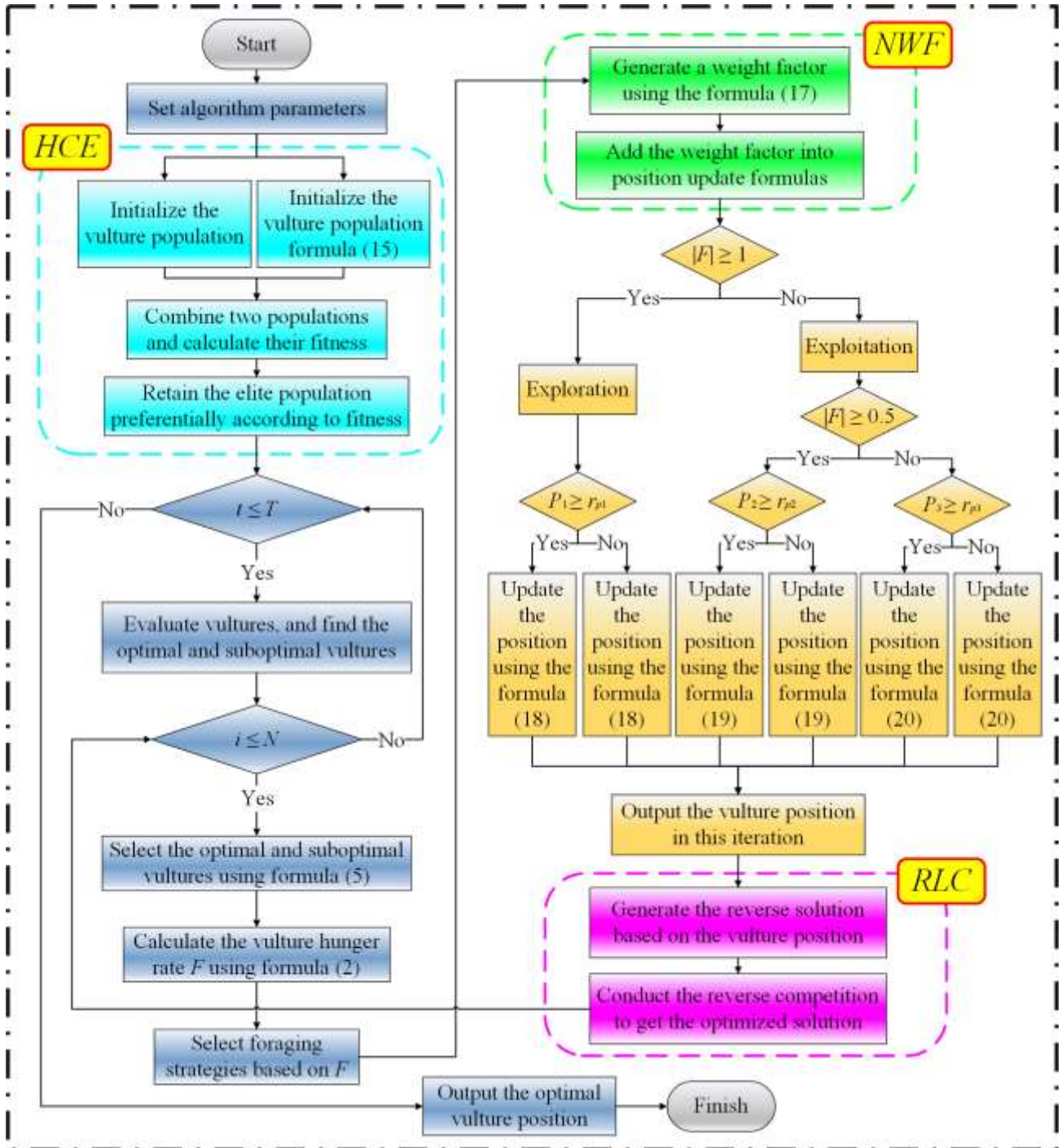


Fig. 4. The flowchart of HWEAVOA.

Table 1. The pseudo-code of HWEAVOA.

Input: The population size N , maximum number of iterations T , parameters used to determine each strategy's choosing $P_1 P_2 P_3$, the selection factors for the initial optimal vulture $a \beta$, parameter with a fixed number W , Henon chaotic mapping parameters $a b$

Output: The position of Vulture and its fitness value

Initialize the golden jackal population $P_i (i = 1, 2, \dots, N)$

Sub-Algorithm 1: Henon chaotic mapping theory and elite population strategy

Calculate the chaotic mapped initialized population using Eq (15)

Combine the chaotic mapped initialized population and the conventional initialized population, calculate the fitness of vultures, and obtain the elite population

while $t=1$ to T

Set $BestV_1$ and $BestV_2$ as the position of the optimal vulture and suboptimal vulture

for (each Vulture (P_i)) do

 Select $R(i)$ using Eq (5)

 Update the F using Eq (2)

Sub-Algorithm 2: Nonlinear adaptive incremental inertial weight factor

Obtain the weight factor using Eq (17), introduced it into the position update formulas of vultures

if ($|F| \geq 1$) (Exploration phase) then

 Update the vulture's location using Eq (18)

else ($|F| < 1$) (Exploitation phase) then

if ($|F| \geq 0.5$) then

 Update the vulture's location using Eq (19)

else ($|F| < 0.5$) then

 Update the vulture's location using Eq (20)

end if

end if

Sub-Algorithm 3: Reverse learning competition strategy

Generate reverse learning solutions using Eq (21)

Decide whether to update the location of the vulture according to the fitness of the reverse learning solutions and the original solutions

end for

end while

Return P_{BestV_1}

4. Experimental results and discussion

Test experiments based on classical and CEC2022 test functions are carried out to validate the performance of the HWEAVOA in this section. The mathematical expressions and function characteristics of classical and CEC2022 test functions are given in Appendix 1 and Appendix 2 respectively.

All experiments were conducted over Windows 10 (64 bit) that runs on CPU Core i7 with 16GB RAM, and Matlab2021a are utilized. In order to minimize the randomness of the algorithm, each algorithm accumulates 1000 tests on the classical test functions, and the population size and maximum number of iterations for all algorithms are set to 30 and 500. In the CEC2022, each algorithm accumulates 30 tests, the population size is set to 20, and the maximum number of iterations for all algorithms is set to 200000 and 1,000,000 respectively in the condition of 10 and 20 dimensions.

The test functions are tested by these algorithms, and the search performance and optimize performance of each algorithm are detected by comparing the test results with the optimal value of the functions. The results mainly contain average (Avg) and standard deviation (Std), where the average (Avg) can verify the optimization ability of the algorithm, the standard deviation (Std) can verify the stability of the optimization process of the algorithm. The data shown in Table 2, Table 4, Table 5, Table 6, Table 7, Table 8, Table 9, Table 10, Table 11, Table 12, Table 13 and Table 14 are the results of the comparison optimization algorithms in solving these benchmark function problems.

In this section, HWEAVOA is compared with the original AVOA, 6 AVOA variant algorithms based on three improved strategies, 10 advanced intelligent optimization algorithms to verify that the better optimization performance of the HWEAVOA.

4.1 Parameters tuning and analysis

In HWEAVOA, W (used in Eq. (1)) is mainly used to balance the exploration and development stages of vulture populations, P_1 (used in Eq. (18)), P_2 (used in Eq. (19)), and P_3 (used in Eq. (20)) are mainly used to assist vultures in selecting different behaviours and update their positions. In the original AVOA, the four parameters are derived from AVOA and are set as 2.5, 0.6, 0.4 and 0.6, respectively in AVOA. This section aims to study the effects of different parameters of the algorithm on the performance of HWEAVOA. The value of W is increased from 2 to 3 with a step size of 0.5, the value of P_1 , P_2 , and P_3 are increased from 0.4 to 0.6 with a step size of 0.1. In this paper, the control variable method is adopted, only one parameter is changed in each experiment, and the values of other parameters are set according to the value of AVOA. For example, when the value of W is increased from 2 to 3, the values of P_1 , P_2 , and P_3 is set as 0.6, 0.4 and 0.6; When the value of P_1 increases from 0.4 to 0.6, the values of W , P_2 , and P_3 are set as 2.5, 0.4 and 0.6. **When the value of P_2**

Table 2. Effect of main parameters on HWEAVOA.

		$W=2$	$W=2.5$	$W=3$	$P_1=0.4$	$P_1=0.5$	$P_1=0.6$	$P_2=0.4$	$P_2=0.5$	$P_2=0.6$	$P_3=0.4$	$P_3=0.5$	$P_3=0.6$
F1	Avg	0.0000E+00	0.0000E+00	0.0000E+00	0.0000E+00	0.0000E+00	0.0000E+00	0.0000E+00	0.0000E+00	0.0000E+00	0.0000E+00	0.0000E+00	0.0000E+00
	Std	0.0000E+00	0.0000E+00	0.0000E+00	0.0000E+00	0.0000E+00	0.0000E+00	0.0000E+00	0.0000E+00	0.0000E+00	0.0000E+00	0.0000E+00	0.0000E+00
F2	Avg	0.0000E+00	0.0000E+00	0.0000E+00	0.0000E+00	0.0000E+00	0.0000E+00	0.0000E+00	0.0000E+00	0.0000E+00	0.0000E+00	0.0000E+00	0.0000E+00
	Std	0.0000E+00	0.0000E+00	0.0000E+00	0.0000E+00	0.0000E+00	0.0000E+00	0.0000E+00	0.0000E+00	0.0000E+00	0.0000E+00	0.0000E+00	0.0000E+00
F3	Avg	0.0000E+00	0.0000E+00	0.0000E+00	0.0000E+00	0.0000E+00	0.0000E+00	0.0000E+00	0.0000E+00	0.0000E+00	0.0000E+00	0.0000E+00	0.0000E+00
	Std	0.0000E+00	0.0000E+00	0.0000E+00	0.0000E+00	0.0000E+00	0.0000E+00	0.0000E+00	0.0000E+00	0.0000E+00	0.0000E+00	0.0000E+00	0.0000E+00
F4	Avg	0.0000E+00	0.0000E+00	0.0000E+00	0.0000E+00	0.0000E+00	0.0000E+00	0.0000E+00	0.0000E+00	0.0000E+00	0.0000E+00	0.0000E+00	0.0000E+00
	Std	0.0000E+00	0.0000E+00	0.0000E+00	0.0000E+00	0.0000E+00	0.0000E+00	0.0000E+00	0.0000E+00	0.0000E+00	0.0000E+00	0.0000E+00	0.0000E+00
F5	Avg	2.6883E-02	5.1640E-03	8.2032E-02	3.4354E-02	2.6498E-02	5.1640E-03	5.1640E-03	2.7286E-02	2.6986E-02	1.0865E-01	5.6189E-03	5.1640E-03
	Std	6.9549E-01	9.3618E-06	2.1932E+00	3.0921E-05	4.0078E-05	9.3618E-06	9.3618E-06	7.3920E-01	7.2193E-01	2.9081E+00	4.9402E-05	9.3618E-06
F5	Avg	3.8864E-04	5.5716E-07	7.3568E-04	5.9363E-04	8.9553E-05	5.5716E-07	5.5716E-07	2.2349E-04	4.3761E-04	5.7315E-04	1.5798E-04	5.5716E-07
	Std	3.3269E-05	7.2768E-13	1.6135E-04	1.3124E-04	1.0231E-07	7.2768E-13	7.2768E-13	2.3907E-06	2.9959E-05	7.6346E-05	9.2823E-07	7.2768E-13
F7	Avg	1.1157E-04	1.2076E-05	1.2361E-04	1.2897E-04	1.2638E-04	1.2076E-05	1.2076E-05	1.2369E-04	1.2223E-04	1.2228E-04	1.2828E-04	1.2076E-05
	Std	1.3064E-08	1.4328E-09	1.3922E-08	1.3623E-08	1.4328E-09	1.4328E-09	1.4328E-09	1.4890E-08	1.2846E-08	1.4201E-08	1.4353E-08	1.4328E-09
F8	Avg	-1.2231E+04	-1.2527E+04	-1.2211E+04	-1.2140E+04	-1.2166E+04	-1.2527E+04	-1.2527E+04	-1.2234E+04	-1.2284E+04	-1.2184E+04	-1.2233E+04	-1.2527E+04
	Std	4.1838E+05	8.6230E+03	4.0985E+05	5.5995E+05	5.0951E+05	8.6230E+03	8.6230E+03	4.0300E+05	2.7943E+05	5.1486E+05	3.9926E+05	8.6230E+03
F9	Avg	0.0000E+00	0.0000E+00	0.0000E+00	0.0000E+00	0.0000E+00	0.0000E+00	0.0000E+00	0.0000E+00	0.0000E+00	0.0000E+00	0.0000E+00	0.0000E+00
	Std	0.0000E+00	0.0000E+00	0.0000E+00	0.0000E+00	0.0000E+00	0.0000E+00	0.0000E+00	0.0000E+00	0.0000E+00	0.0000E+00	0.0000E+00	0.0000E+00
F10	Avg	8.8818E-16	8.8818E-16	8.8818E-16	8.8818E-16	8.8818E-16	8.8818E-16	8.8818E-16	8.8818E-16	8.8818E-16	8.8818E-16	8.8818E-16	8.8818E-16
	Std	0.0000E+00	0.0000E+00	0.0000E+00	0.0000E+00	0.0000E+00	0.0000E+00	0.0000E+00	0.0000E+00	0.0000E+00	0.0000E+00	0.0000E+00	0.0000E+00
F11	Avg	0.0000E+00	0.0000E+00	0.0000E+00	0.0000E+00	0.0000E+00	0.0000E+00	0.0000E+00	0.0000E+00	0.0000E+00	0.0000E+00	0.0000E+00	0.0000E+00
	Std	0.0000E+00	0.0000E+00	0.0000E+00	0.0000E+00	0.0000E+00	0.0000E+00	0.0000E+00	0.0000E+00	0.0000E+00	0.0000E+00	0.0000E+00	0.0000E+00
F12	Avg	3.8504E-05	5.7613E-09	6.4453E-05	2.2367E-05	3.2174E-05	5.7613E-09	5.7613E-09	3.9925E-05	3.7442E-05	6.3313E-05	4.4636E-05	5.7613E-09
	Std	1.6973E-07	2.5338E-15	3.1122E-07	3.1268E-08	1.3129E-07	2.5338E-15	2.5338E-15	1.2126E-07	1.6751E-07	3.9589E-07	1.4654E-07	2.5338E-15

F13	Avg	2.5268E-05	7.3758E-08	5.6365E-05	1.1599E-05	4.0506E-05	7.3758E-08	7.3758E-08	5.3111E-05	1.4429E-04	2.7472E-04	3.3519E-04	7.3758E-08
	Std	2.5417E-07	1.1564E-14	6.1552E-07	1.2537E-07	5.5799E-07	1.1564E-14	1.1564E-14	6.4852E-06	1.1973E-05	1.6274E-05	3.1603E-05	1.1564E-14
F14	Avg	1.6271E+00	1.2568E+00	1.6300E+00	1.6292E+00	1.6331E+00	1.2568E+00	1.2568E+00	1.6647E+00	1.7016E+00	1.6729E+00	1.6351E+00	1.2568E+00
	Std	8.1281E-01	4.2014E-01	8.1418E-01	7.5186E-01	7.5475E-01	4.2014E-01	4.2014E-01	8.6754E-01	8.1706E-01	7.5072E-01	7.7219E-01	4.2014E-01
F15	Avg	6.0018E-04	3.1114E-04	4.8056E-04	4.7329E-04	6.1174E-04	3.1114E-04	3.1114E-04	4.8231E-04	4.7794E-04	6.2905E-04	6.1847E-04	3.1114E-04
	Std	5.7123E-08	5.9227E-09	4.2229E-08	4.2130E-08	6.4023E-08	5.9227E-09	5.9227E-09	3.9255E-08	3.7585E-08	6.3280E-08	6.0363E-08	5.9227E-09
F16	Avg	-1.0316E+00	-1.0316E+00	-1.0316E+00	-1.0316E+00	-1.0316E+00	-1.0316E+00	-1.0316E+00	-1.0316E+00	-1.0316E+00	-1.0316E+00	-1.0316E+00	-1.0316E+00
	Std	3.7659E-28	2.0454E-28	3.6468E-28	4.1299E-27	8.8193E-28	2.0454E-28	2.0454E-28	9.4225E-26	2.0568E-22	5.3015E-27	1.8193E-26	2.0454E-28
F17	Avg	3.9789E-01	3.9789E-01	3.9789E-01	3.9789E-01	3.9789E-01	3.9789E-01	3.9789E-01	3.9789E-01	3.9789E-01	3.9789E-01	3.9789E-01	3.9789E-01
	Std	6.4879E-28	5.4939E-28	2.6873E-27	1.3948E-27	6.4956E-28	5.4939E-28	5.4939E-28	1.1243E-25	7.6632E-23	1.3581E-19	6.5868E-20	5.4939E-28
F18	Avg	3.2166E+00	3.0270E+00	3.1626E+00	3.2703E+00	3.0815E+00	3.0270E+00	3.0270E+00	3.4059E+00	3.3792E+00	3.2974E+00	3.2169E+00	3.0270E+00
	Std	5.7851E+01	7.2827E-10	4.3476E+01	7.2169E+01	2.1804E+01	7.2827E-10	7.2827E-10	1.0770E+01	1.0062E+01	7.9305E-01	5.7851E+01	7.2827E-10
F19	Avg	-3.8628E+00	-3.8628E+00	-3.8628E+00	-3.8628E+00	-3.8628E+00	-3.8628E+00	-3.8628E+00	-3.8628E+00	-3.8628E+00	-3.8628E+00	-3.8628E+00	-3.8628E+00
	Std	1.4141E-14	8.6647E-15	8.1016E-14	1.2650E-14	1.5864E-14	8.6647E-15	8.6647E-15	4.3868E-10	2.6346E-07	1.1324E-14	1.1343E-13	8.6647E-15
F20	Avg	-3.2751E+00	-3.2713E+00	-3.2749E+00	-3.2772E+00	-3.2726E+00	-3.2713E+00	-3.2713E+00	-3.2745E+00	-3.2773E+00	-3.2766E+00	-3.2751E+00	-3.2713E+00
	Std	3.4463E-03	3.5391E-03	3.4545E-03	3.6469E-03	3.6189E-03	3.5391E-03	3.5391E-03	3.5159E-03	3.5241E-03	3.4363E-03	3.4358E-03	3.5391E-03
F21	Avg	-1.0153E+01	-1.0153E+01	-1.0153E+01	-1.0153E+01	-1.0153E+01	-1.0153E+01	-1.0153E+01	-1.0153E+01	-1.0153E+01	-1.0153E+01	-1.0153E+01	-1.0153E+01
	Std	2.7364E-20	1.9212E-20	3.2065E-20	5.3411E-20	8.9653E-20	1.9212E-20	1.9212E-20	2.3969E-18	2.7226E-15	3.1640E-13	2.4321E-13	1.9212E-20
F22	Avg	-1.0403E+01	-1.0402E+01	-1.0403E+01	-1.0403E+01	-1.0403E+01	-1.0402E+01	-1.0402E+01	-1.0403E+01	-1.0403E+01	-1.0403E+01	-1.0403E+01	-1.0402E+01
	Std	6.1829E-20	5.5748E-20	5.6164E-20	1.4156E-19	7.5138E-20	5.5748E-20	5.5748E-20	1.9467E-18	6.0416E-16	5.0390E-13	4.0150E-13	5.5748E-20
F23	Avg	-1.0536E+01	-1.0536E+01	-1.0536E+01	-1.0536E+01	-1.0536E+01	-1.0536E+01	-1.0536E+01	-1.0536E+01	-1.0536E+01	-1.0536E+01	-1.0536E+01	-1.0536E+01
	Std	5.4597E-20	3.9712E-20	4.6431E-20	2.0897E-19	8.4799E-20	3.9712E-20	3.9712E-20	2.4598E-18	1.2705E-16	2.8091E-13	3.1066E-13	3.9712E-20

2

3

4 increases from 0.4 to 0.6, the values of W , P_1 , and P_3 are set as 2.5, 0.6 and 0.6. When the value of P_3
5 increases from 0.4 to 0.6, the values of W , P_1 , and P_2 are set as 2.5, 0.6 and 0.4. The effects of different
6 parameters on the performance of HWEAVOA are shown in Table 2.

7 The results show that HWEAVOA has the highest search ability and algorithm stability when
8 the values of W , P_1 , P_2 , and P_3 are set as 2.5, 0.6, 0.4 and 0.6, respectively. Therefore, the HWEAVOA
9 selects the same parameter settings as the AVOA in this paper.

10 Based on the above-mentioned analysis, the main parameters of HWEAVOA and its variant
11 algorithms are shown as Table 3.

12 Table 3. The parameter settings.

Algorithm	Time/Year	Value
GA	1980	$P_c=0.8, P_m=0.1$
PSO	1995	Inertia factor = 0.3, $c_1 = 1, c_2 = 1$
DE	1997	Scaling factor = 0.5, Crossover probability = 0.5
GWO	2014	$a = [2,0]$
COOT	2021	/
RSO	2021	$R = \text{floor}((5-1) \times \text{rand}(1,1) + 1)$
GTO	2021	$p=0.03, \beta = 3, \omega = 0.8$
AOA	2019	$E_0 = [-1,1]$
AVOA	2021	$p_1 = 0.6, p_2 = 0.4, p_3 = 0.6, \alpha = 0.8, \beta = 0.2, \gamma = 2.5$
IHAOAVOA	2022	$p_1 = 0.6, p_2 = 0.4, p_3 = 0.6, \alpha = 0.8, \beta = 0.2, \gamma = 2.5, U = 0.00565, r_1 = 10,$ $\omega = 0.005, \theta = 1.5\pi$
OAVOA	2022	$L_1=0.8, L_2=0.2, w = 2.0, p_1 = 0.5, p_2 = 0.5, p_3 = 0.5$
HAVOA	/	$p_1 = 0.6, p_2 = 0.4, p_3 = 0.6, \alpha = 0.8, \beta = 0.2, W = 2.5, a=1.4, b=0.3$
WAVOA	/	$p_1 = 0.6, p_2 = 0.4, p_3 = 0.6, \alpha = 0.8, \beta = 0.2, W = 2.5$
EAVOA	/	$p_1 = 0.6, p_2 = 0.4, p_3 = 0.6, \alpha = 0.8, \beta = 0.2, W = 2.5$
HWAVOA	/	$p_1 = 0.6, p_2 = 0.4, p_3 = 0.6, \alpha = 0.8, \beta = 0.2, W = 2.5, a=1.4, b=0.3$
HEAVOA	/	$p_1 = 0.6, p_2 = 0.4, p_3 = 0.6, \alpha = 0.8, \beta = 0.2, W = 2.5, a=1.4, b=0.3$
WEAVOA	/	$p_1 = 0.6, p_2 = 0.4, p_3 = 0.6, \alpha = 0.8, \beta = 0.2, W = 2.5$
HWEAVOA	/	$p_1 = 0.6, p_2 = 0.4, p_3 = 0.6, \alpha = 0.8, \beta = 0.2, W = 2.5, a=1.4, b=0.3$

13 4.2 Effects of HCE, NWF and RLC

14 To study the optimization performance of the HWEAVOA algorithm, three improved strategies
15 (HCE, NWF and RLC) are introduced in the optimization process of HWEAVOA. In this section, we

16 focus on the impact of the three improvement strategies on the original AVOA. The three
17 improvement strategies are named briefly with "H", "W", and "E". The performance of HWEAVOA,
18 6 variants of AVOA: HAVOA, WAVOA, EAVOA, HWAVOA, HEAVOA, WEAVOA and AVOA is
19 tested.

20 HAVOA, WAVOA and EAVOA represent the introduction of HCE, NWF and RLC into the
21 original AVOA algorithm respectively. HWAVOA means the introduction of both HCE and NWF into
22 the original AVOA algorithm. HEAVOA means to the introduction of both HCE and RLC into the
23 original AVOA algorithm. WEAVOA means to the introduction of both NWF and RLC into the
24 original AVOA algorithm. The parameter settings of these variant algorithms are shown in Table 3.

25 As shown in Table 4, the experimental results show that the optimal value of functions, F1~F4
26 can be obtained by HWEAVOA in unimodal benchmark functions. For multimodal benchmark
27 functions, the optimal values of functions F8 and F11 can be obtained by HWEAVOA, while the
28 optimal value found by HWEAVOA is the best of all algorithms on other multimodal benchmark
29 functions. For fixed-dimension multimodal benchmark functions, the optimal values of functions F16,
30 F17, F19, F21, F22 and F23 can be obtained by HWEAVOA, while HWEAVOA performs better on
31 other fixed-dimensional multimodal benchmark functions than different algorithms.

32 As shown in Fig. 5, some convergence curves are displayed in 0~50 generations to show the
33 difference in iterative efficiency more clearly and intuitively. When HWEAVOA solves F1 and F4,
34 the convergence speed of the HWEAVOA algorithm is close to WAVOA, HWAVOA, and WEAVOA,
35 which is significantly faster than HAVOA, EVOA. In the process of solving F6 ~ F8, F12, F13 and
36 F15, the convergence speed of HWEAVOA is slightly faster than other variant algorithms. When
37 solving F9, the optimal value is obtained around 30 times by all algorithms, but the convergence rate
38 of HWEAVOA is still the fastest. When solving F21 and F23, the convergence speeds of HAVOA,
39 EAVOA, HEAVOA, WEAVOA, AVOA and HWEAVOA are significantly faster than those of
40 WAVOA and HWAVOA. Meanwhile, in HAVOA, EAVOA, HEAVOA, WEAVOA, AVOA and
41 HWEAVOA, the convergence speed of HWEAVOA is slightly faster than those of HAVOA, EAVOA,
42 HEAVOA, WEAVOA and AVOA. In summary, HWEAVOA has the advantage of the convergence
43 speed and precision in the process of solving the classical test functions compared with other variants.

Table 4. The comparison results of HWEAVOA and its variant algorithms based on 23 classical functions.

		AVOA	HAVOA	WAVOA	EAVOA	HWAVOA	HEAVOA	WEAVOA	HWEAVOA
F1	Avg	1.9963E-153	2.5018E-148	0.0000E+00	4.0257E-158	0.0000E+00	2.5129E-148	0.0000E+00	0.0000E+00
	Std	2.4765E-303	6.2219E-293	0.0000E+00	3.8824E-313	0.0000E+00	6.2917E-293	0.0000E+00	0.0000E+00
F2	Avg	3.8867E-82	8.4219E-82	0.0000E+00	3.9294E-78	0.0000E+00	7.8591E-82	0.0000E+00	0.0000E+00
	Std	1.2054E-160	4.6613E-160	0.0000E+00	1.5256E-152	0.0000E+00	5.9964E-160	0.0000E+00	0.0000E+00
F3	Avg	8.9768E-102	5.4945E-110	0.0000E+00	2.1168E-107	0.0000E+00	7.6219E-114	0.0000E+00	0.0000E+00
	Std	8.0424E-200	8.6277E-217	0.0000E+00	4.4617E-211	0.0000E+00	5.7274E-224	0.0000E+00	0.0000E+00
F4	Avg	2.2498E-79	7.4318E-74	0.0000E+00	1.2061E-77	0.0000E+00	1.3964E-75	0.0000E+00	0.0000E+00
	Std	2.9731E-155	5.5111E-144	0.0000E+00	1.0767E-151	0.0000E+00	9.5524E-148	0.0000E+00	0.0000E+00
F5	Avg	1.0696E-01	1.8466E-01	9.5919E-01	8.0085E-02	8.4488E-01	5.3555E-02	2.7484E-02	5.1640E-03
	Std	2.8334E+00	4.9171E+00	2.5307E+01	2.1173E+00	2.2462E+01	1.4159E+00	7.1551E-01	9.3618E-06
F6	Avg	9.4805E-04	6.9788E-04	4.8070E-03	4.2223E-06	3.6125E-03	4.3258E-06	9.9471E-04	5.5716E-07
	Std	2.1433E-04	1.4511E-04	7.8387E-04	2.1634E-11	5.6410E-04	1.6394E-11	1.7106E-04	7.2768E-13
F7	Avg	2.6506E-04	2.7468E-04	1.2182E-04	2.6274E-04	1.1248E-04	2.8227E-04	1.1858E-04	1.2076E-05
	Std	8.6811E-08	8.2349E-08	1.5128E-08	7.0647E-08	1.2867E-08	8.8468E-08	1.4729E-08	1.4328E-09
F8	Avg	-1.2259E+04	-1.2360E+04	-1.1980E+04	-1.1904E+04	-1.2227E+04	-1.2200E+04	-1.1452E+04	-1.2527E+04
	Std	3.3662E+05	82.4518E+05	7.3254E+05	7.6739E+05	3.6306E+05	4.9240E+05	1.2462E+06	8.6230E+03
F9	Avg	0.0000E+00	0.0000E+00	0.0000E+00	0.0000E+00	0.0000E+00	0.0000E+00	0.0000E+00	0.0000E+00
	Std	0.0000E+00	0.0000E+00	0.0000E+00	0.0000E+00	0.0000E+00	0.0000E+00	0.0000E+00	0.0000E+00
F10	Avg	8.8818E-16	8.8818E-16	8.8818E-16	8.8818E-16	8.8818E-16	8.8818E-16	8.8818E-16	8.8818E-16
	Std	0.0000E+00	0.0000E+00	0.0000E+00	0.0000E+00	0.0000E+00	0.0000E+00	0.0000E+00	0.0000E+00
F11	Avg	0.0000E+00	0.0000E+00	0.0000E+00	0.0000E+00	0.0000E+00	0.0000E+00	0.0000E+00	0.0000E+00
	Std	0.0000E+00	0.0000E+00	0.0000E+00	0.0000E+00	0.0000E+00	0.0000E+00	0.0000E+00	0.0000E+00
F12	Avg	4.9655E-05	2.8069E-05	2.0457E-04	1.8675E-07	2.7246E-04	1.9578E-07	5.3324E-05	5.7613E-09
	Std	3.6391E-07	1.3827E-07	1.4639E-06	2.3942E-14	2.2589E-06	3.3657E-14	2.2817E-07	2.5338E-15

F13	Avg	1.1214E-04	2.5308E-04	7.4559E-04	1.2567E-05	8.2935E-04	1.2357E-05	4.4779E-04	7.3758E-08
	Std	1.0033E-05	2.0079E-05	1.0026E-04	1.2832E-07	3.3927E-04	1.4658E-07	2.5079E-05	1.1564E-14
F14	Avg	1.6611E+00	1.6072E+00	1.9801E+00	1.4069E+00	1.9191E+00	1.3196E+00	1.6598E+00	1.2568E+00
	Std	2.6207E+00	2.2397E+00	4.4085E+00	5.4571E-01	4.1545E+00	4.4978E-01	8.0963E-01	4.2014E-01
F15	Avg	4.8436E-04	4.9354E-04	5.9508E-04	4.7545E-04	5.9045E-04	4.8459E-04	6.0704E-04	3.1114E-04
	Std	4.3216E-08	4.6153E-08	4.8267E-08	4.4021E-08	4.9211E-08	4.4568E-08	5.7868E-08	5.9227E-09
F16	Avg	-1.0316E+00	-1.0316E+00	-1.0316E+00	-1.0316E+00	-1.0316E+00	-1.0316E+00	-1.0316E+00	-1.0316E+00
	Std	2.0127E-27	1.3822E-27	3.5962E-19	6.4619E-28	9.3261E-20	2.4523E-27	4.5714E-19	2.0454E-28
F17	Avg	3.9789E-01	3.9789E-01	3.9789E-01	3.9789E-01	3.9789E-01	3.9789E-01	3.9789E-01	3.9789E-01
	Std	1.1963E-27	6.1753E-28	2.9267E-19	8.8214E-28	2.3144E-19	9.8867E-28	1.1516E-19	5.4939E-28
F18	Avg	3.0540E+00	3.0813E+00	3.6767E+00	3.0000E+00	3.2166E+00	3.0000E+00	3.1084E+00	3.0270E+00
	Std	1.4551E+00	2.1804E+00	2.6518E+01	7.0034E+00	5.7851E+00	4.9928E-10	2.9043E+00	7.2827E-10
F19	Avg	-3.8627E+00	-3.8627E+00	-3.8621E+00	-3.8628E+00	-3.8628E+00	-3.8628E+00	-3.8628E+00	-3.8628E+00
	Std	3.3896E-07	2.8124E-15	4.0078E-06	2.3961E-14	3.2387E-06	4.5639E-15	1.5848E-14	8.6647E-15
F20	Avg	-3.2721E+00	-3.2744E+00	-3.2563E+00	-3.2746E+00	-3.2600E+00	-3.2729E+00	-3.2700E+00	-3.2713E+00
	Std	3.7345E-03	3.5764E-03	8.0432E-03	3.3988E-03	1.0064E-02	3.3433E-03	3.5417E-03	3.5391E-03
F21	Avg	-1.0153E+01	-1.0153E+01	-1.0153E+01	-1.0153E+01	-1.0153E+01	-1.0153E+01	-1.0153E+01	-1.0153E+01
	Std	4.7988E-20	2.0407E-20	2.8514E-01	2.8657E-20	2.7672E-01	4.2593E-19	6.0129E-13	1.9212E-20
F22	Avg	-1.0402E+01	-1.0402E+01	-1.0402E+01	-1.0402E+01	-1.0402E+01	-1.0402E+01	-1.0402E+01	-1.0402E+01
	Std	2.4459E-20	5.5798E-20	5.5694E-01	4.0875E-20	3.8749E-01	1.6657E-20	7.1757E-13	5.5748E-20
F23	Avg	-1.0536E+01	-1.0536E+01	-1.0536E+01	-1.0536E+01	-1.0536E+01	-1.0536E+01	-1.0536E+01	-1.0536E+01
	Std	5.0758E-20	5.2697E-20	4.3976E-01	6.7956E-20	2.9312E-01	5.6657E-20	5.3071E-13	3.9712E-20

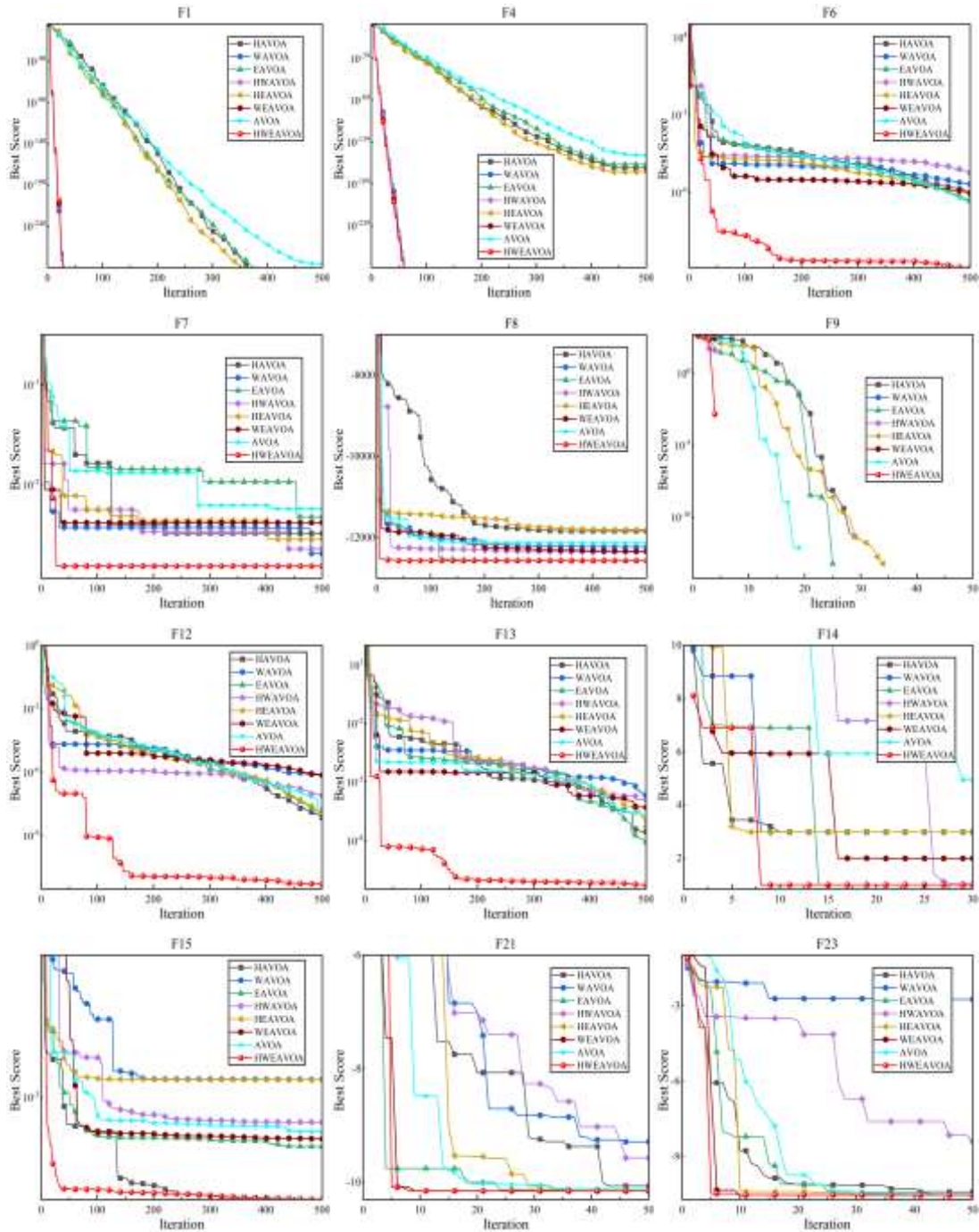


Fig. 5. Convergence curves of HWEAVOA and its variant algorithms based on F1, F4, F6, F7, F8, F9, F12, F13, F14, F15, F21 and F23.

4.3 Evaluation with the classical test functions

The performance of HWEAVOA is compared with 10 advanced intelligent optimization algorithms to verify the superiority, including GA (Deng, Zhang, et al., 2022), PSO (Cheng & Jin, 2015), DE (Das & Suganthan, 2011), GWO (Mirjalili, Mirjalili, & Lewis, 2014), COOT (Naruei & Keynia, 2021), RSO (Dhiman, Garg, Nagar, Kumar, & Dehghani, 2021), ATO (Naruei & Keynia,

57 2021), AOA (Abualigah, Diabat, Mirjalili, Abd Elaziz, & Gandomi, 2021), IHAOAVOA (Xiao, et al.,
58 2022) and OAVOA (Jena, Naik, Panda, & Abraham, 2022). The parameter settings of the algorithms
59 are shown in Table 3. The comparative results of these algorithms based on the 23 functions are shown
60 in Table 5. For fairness, all used optimization methods run in the same test conditions.

61 The experimental results in Table 5 present that the HWEAVOA ranks first in 18 test functions
62 of F1~F7, F9~F12, F15~F17, F19, and F21~F23, including seven unimodal benchmark functions,
63 four multimodal benchmark functions and seven fixed-dimension multimodal benchmark functions.
64 The performance of the HWEAVOA in classical test functions indicates its ability in solving real-
65 world optimization problems. Especially for the IHAOAVOA and OAVOA, the HWEAVOA
66 performs better than IHAOAVOA in 7 benchmark functions, including F5~F8, F12 F15 and F18, and
67 better than OAVOA in F1~F7, F12, F13 and F15, which benefiting from the NWF strategy balances
68 the exploration and exploitation capabilities, it is like a powerful engine that drives the HWEAVOA
69 to excavate small areas effectively.

70 In order to have a more obvious analysis, the Friedman test is used to compare the solution
71 results of the above algorithms. As shown in Table 6, the overall average ranking of HWEAVOA is
72 1.70, lower than the 1.96 of IHAOAVOA and the 2.43 of OAVOA. Meanwhile, it is evident that the
73 HWEAVOA bestows a much faster convergence speed than other advanced algorithms as shown in
74 Fig. 6. When solving F1, F3, F5, F7, F12 and F13, the HWEAVOA algorithm converges the fastest,
75 followed by IHAOAVOA, and significantly faster than the other advanced algorithms, which means
76 that it reaches to the best area very fast. It shows that the search performance, solution precision and
77 the convergence velocity of the HWEAVOA are significantly enhanced. These features mean that the
78 HWEAVOA has a robust global search capability, making an appropriate balance between the search
79 mechanisms.

Table 5. The comparison results of HWEAVOA and other advanced algorithms based on 23 classical functions.

		GA	PSO	DE	GWO	COOT	RSO	GTO	AOA	IHAOAVOA	OAVOA	HWEAVOA
F1	Avg	4.1042E+04	1.2250E+01	3.6098E+04	4.7134E-15	2.7198E-08	8.6636E-248	6.0837E-220	4.8743E-10	0.0000E+00	1.3217E-214	0.0000E+00
	Std	3.1080E+07	1.5256E+03	5.4347E+07	6.5329E-29	3.4832E-13	0.0000E+00	0.0000E+00	1.3742E-16	0.0000E+00	0.0000E+00	0.0000E+00
F2	Avg	1.8851E+13	6.2036E+00	2.3112E+07	1.5543E-09	1.6678E-05	5.2416E-138	7.4023E-114	6.9967E-186	0.0000E+00	4.3159E-117	0.0000E+00
	Std	1.6312E+28	4.2789E+00	2.9810E+16	9.4647E-19	8.4832E-08	8.2089E-273	1.3868E-224	0.0000E+00	0.0000E+00	1.8628E-230	0.0000E+00
F3	Avg	1.1237E+05	7.0413E+03	6.9524E+04	6.8183E-02	1.7416E-06	2.7439E-89	9.5042E-208	9.7847E-03	0.0000E+00	1.4899E-189	0.0000E+00
	Std	8.0911E+08	2.7818E+07	2.4865E+08	3.0893E-02	3.0127E-09	7.5145E-175	0.0000E+00	3.9430E+04	0.0000E+00	0.0000E+00	0.0000E+00
F4	Avg	6.7858E+01	3.3038E+00	8.6647E+01	9.4083E-04	1.2834E-04	2.4997E-35	1.0824E-113	3.0869E-02	0.0000E+00	5.8533E-106	0.0000E+00
	Std	1.8298E+01	1.2591E+00	1.8375E+01	6.0127E-07	6.2719E-06	6.2148E-67	1.4027E-224	3.5147E-04	0.0000E+00	3.3842E-208	0.0000E+00
F5	Avg	1.4811E+08	2.2561E+02	1.0701E+08	2.7391E+01	6.6792E+01	2.8826E+01	4.5404E+00	2.8567E+01	2.1256E-01	5.4877E-02	5.1640E-03
	Std	9.6595E+14	1.8096E+04	1.8578E+15	6.0839E-01	9.0176E+03	3.9817E-02	9.4188E+01	6.5634E-02	5.6026E+00	1.4621E+00	9.3618E-06
F6	Avg	4.1204E+04	1.1588E+01	3.6279E+04	1.0079E+01	1.1245E+00	3.4098E+00	7.1435E-05	3.5097E+00	3.9115E-06	3.7343E-05	5.5716E-07
	Std	2.9506E+07	9.3303E+02	5.5716E+07	1.8281E-01	1.0970E+00	2.4009E-01	3.9127E-08	8.1452E-02	5.1962E-11	2.0141E-06	7.2768E-13
F7	Avg	7.5735E+01	7.2691E-01	4.8078E+01	3.7954E-03	8.6162E-03	4.7203E-04	1.6827E-04	1.1423E-04	6.0195E-05	3.3083E-04	1.2076E-05
	Std	2.4761E+02	9.3997E-02	3.6733E+02	3.9015E-06	5.1927E-05	3.3459E-07	1.9676E-08	1.2764E-08	3.8296E-09	1.2611E-07	1.4328E-09
F8	Avg	-5.3712E+03	-2.5205E+03	-3.0526E+03	-5.9347E+03	-6.9383E+03	-5.6900E+03	-1.2569E+04	-5.0043E+03	-1.2033E+04	-1.2532E+04	-1.2527E+04
	Std	1.0771E+07	1.5915E+05	1.6331E+05	8.2120E+05	9.0514E+05	1.1531E+06	2.4892E-04	1.8333E+05	1.2818E+06	1.1926E+04	8.6230E+03
F9	Avg	2.9866E+02	6.5850E+01	3.6020E+02	7.9611E+00	2.0334E-05	1.3200E-01	0.0000E+00	0.0000E+00	0.0000E+00	0.0000E+00	0.0000E+00
	Std	5.7275E+02	2.3507E+02	7.1989E+02	4.9283E+01	1.2907E-07	1.7406E+01	0.0000E+00	0.0000E+00	0.0000E+00	0.0000E+00	0.0000E+00
F10	Avg	1.7983E+01	5.7875E+00	1.9674E+01	1.2613E-08	4.4427E-06	1.9959E-02	8.8846E-16	8.8846E-16	8.8818E-16	8.8818E-16	8.8818E-16
	Std	3.6111E-01	1.1971E+00	2.4807E-01	5.9814E-17	1.2249E-08	3.9797E-01	0.0000E+00	0.0000E+00	0.0000E+00	0.0000E+00	0.0000E+00
F11	Avg	3.6948E+02	3.7399E+02	3.2642E+02	7.0424E-03	3.1865E-07	0.0000E+00	0.0000E+00	3.0226E-01	0.0000E+00	0.0000E+00	0.0000E+00
	Std	2.4912E+03	1.1165E+03	4.8491E+03	1.4327E-04	7.0743E-11	0.0000E+00	0.0000E+00	3.7848E-02	0.0000E+00	0.0000E+00	0.0000E+00
F12	Avg	3.4562E+08	2.2401E+00	2.3115E+08	6.0822E-02	2.6490E-01	3.5152E-01	3.4023E-06	5.9888E-01	4.2621E-08	1.6857E-07	5.7613E-09
	Std	6.6870E+15	9.6440E-01	1.6850E+16	1.5193E-03	2.6387E-01	1.7652E-02	5.1433E-11	2.3017E-03	5.0366E-15	7.8192E-14	2.5338E-15

F13	Avg	6.7274E+08	1.7115E+01	4.5862E+08	8.2798E-01	9.3609E-01	2.8840E+00	3.0871E-03	2.8447E+00	7.3259E-08	3.0287E-06	7.3758E-08
	Std	2.1793E+16	5.0229E+01	4.3448E+16	7.1988E-02	3.6735E-01	1.7200E-02	1.0143E-04	9.1592E-03	2.1563E-14	2.3512E-11	1.1564E-14
F14	Avg	3.5323E+00	1.5661E+00	6.0050E+00	4.7868E+00	1.1190E+00	2.8793E+00	9.9800E-01	9.8511E+00	1.1240E+00	1.1450E+00	1.2568E+00
	Std	5.2759E+00	1.6942E+00	1.5198E+01	1.7402E+01	5.4012E-01	5.3491E+00	3.1427E-14	1.5635E+01	2.2331E-01	1.6562E-01	4.2014E-01
F15	Avg	6.9147E-02	1.4523E-03	1.1645E-02	4.8843E-03	1.4215E-03	1.2709E-03	4.3286E-04	1.9243E-02	3.2956E-04	3.4519E-04	3.1114E-04
	Std	5.7091E-03	2.0914E-05	6.9245E-05	6.8234E-05	1.3566E-05	4.1096E-06	9.8458E-08	8.0452E-04	5.1782E-09	1.3427E-08	5.9227E-09
F16	Avg	-1.0316E+00	-1.0316E+00	-1.0073E+00	-1.0316E+00	-1.0316E+00	-1.0314E+00	-1.0316E+00	-1.0316E+00	-1.0316E+00	-1.0316E+00	-1.0316E+00
	Std	2.0421E-20	4.9449E-02	8.2801E-04	8.9123E-32	5.4623E-15	1.0546E-06	1.4023E-08	1.0924E-31	2.5641E-31	2.4987E-18	2.0454E-28
F17	Avg	4.0333E-01	3.9923E-01	5.5624E-01	3.9789E-01	3.9789E-01	3.9789E-01	3.9789E-01	3.9789E-01	3.9789E-01	3.9789E-01	3.9789E-01
	Std	3.8374E-12	4.5679E-03	4.7895E-02	1.2345E-05	0.0000E+00	0.0000E+00	0.0000E+00	0.0000E+00	0.0000E+00	3.2654E-08	7.3978E-08
F18	Avg	1.5813E+01	3.5473E+00	3.7994E+00	3.6481E+00	3.0000E+00	3.0001E+00	3.0000E+00	1.3381E+01	3.7290E+00	3.0000E+00	3.0270E+00
	Std	1.4722E+02	2.7410E+01	3.0565E+00	5.2068E+01	6.9277E-19	2.3944E-08	2.1145E-30	2.8020E+02	1.9151E+01	4.6328E-14	7.2827E-10
F19	Avg	-3.8616E+00	-3.8609E+00	-3.8465E+00	-3.8614E+00	-3.8627E+00	-3.4179E+00	-3.8627E+00	-3.8497E+00	-3.8628E+00	-3.8628E+00	-3.8628E+00
	Std	1.9023E-06	8.3956E-04	4.2195E-04	5.1753E-06	4.5023E-19	1.3269E-01	1.4459E-30	3.3421E-05	4.7624E-18	8.5026E-12	8.6647E-15
F20	Avg	-3.2653E+00	-3.2493E+00	-2.8880E+00	-3.2590E+00	-3.2921E+00	-1.7429E+00	-3.2763E+00	-3.0254E+00	-3.2731E+00	-3.2813E+00	-3.2713E+00
	Std	3.4172E-03	1.1971E-02	3.4913E-02	6.8934E-03	2.6569E-03	2.9658E-01	3.3445E-03	1.2822E-02	3.4848E-03	3.1829E-03	3.5391E-03
F21	Avg	-5.7021E+00	-5.6647E+00	-2.1978E+00	-8.9422E+00	-8.4477E+00	-7.7425E-01	-1.0153E+01	-3.7305E+00	-1.0153E+01	-1.0153E+01	-1.0153E+01
	Std	1.0379E+01	1.0981E+01	1.1273E+00	5.9845E+00	8.8103E+00	3.5984E-01	2.6654E-30	1.8135E+00	1.5897E-20	9.2574E-14	1.9212E-20
F22	Avg	-5.8522E+00	-5.9267E+00	-2.4080E+00	-1.0209E+01	-9.5557E+00	-1.0310E+01	-1.4029E+01	-3.7478E+00	-1.4029E+01	-1.4029E+01	-1.4029E+01
	Std	1.1314E+01	1.1321E+01	1.0497E+00	1.1966E+00	5.1247E+00	5.0322E-01	3.7216E-30	2.2685E+00	3.5447E-20	2.1959E-12	5.5748E-20
F23	Avg	-5.8181E+00	-5.5764E+00	-2.5292E+00	-1.0226E+01	-9.9543E+00	-1.2656E+01	-1.0536E+01	-3.8141E+00	-1.0536E+01	-1.0536E+01	-1.0536E+01
	Std	1.1950E+01	1.2440E+01	1.3680E+00	2.2807E+00	3.8712E+00	5.9897E-01	7.0713E-30	2.8314E+00	4.2365E-13	9.9654E-20	3.9712E-20

Table 6. The Friedman test results based on the classical test functions.

	GA	PSO	DE	GWO	COOT	RSO	GTO	AOA	IHAOAVOA	OAVOA	HWEAVOA
F1	11	9	10	6	8	3	4	7	1	5	1
F2	11	9	10	7	8	4	6	3	1	5	1
F3	11	9	10	8	6	5	3	7	1	4	1
F4	10	9	11	7	6	5	8	3	1	4	1
F5	11	9	10	5	8	7	4	6	3	2	1
F6	11	9	10	5	6	7	4	8	2	3	1
F7	11	9	10	7	8	6	4	3	2	5	1
F8	8	11	10	6	5	7	1	9	4	2	3
F9	10	9	11	8	7	6	1	1	1	1	1
F10	10	9	11	6	7	8	1	1	1	1	1
F11	10	11	9	7	6	1	1	8	1	1	1
F12	11	9	10	5	6	7	4	8	2	3	1
F13	11	9	10	5	6	8	4	7	1	3	2
F14	8	6	10	9	2	7	1	11	3	4	5
F15	11	7	9	8	6	5	4	10	2	3	1
F16	1	1	11	1	1	10	1	1	1	1	1
F17	10	9	11	1	1	1	1	1	1	1	1
F18	11	6	9	7	1	4	1	10	8	1	5
F19	6	8	10	7	4	11	4	9	1	1	1
F20	7	9	2	8	1	11	4	10	5	3	6
F21	7	8	10	5	6	11	1	9	1	1	1
F22	9	8	11	6	7	5	1	10	1	1	1
F23	8	9	11	6	7	5	1	10	1	1	1
Avg. Rank/No.	9.30/10	8.35/9	9.83/11	6.09/6	5.35/5	6.26/7	2.78/4	6.61/8	1.96/2	2.43/3	1.70/1

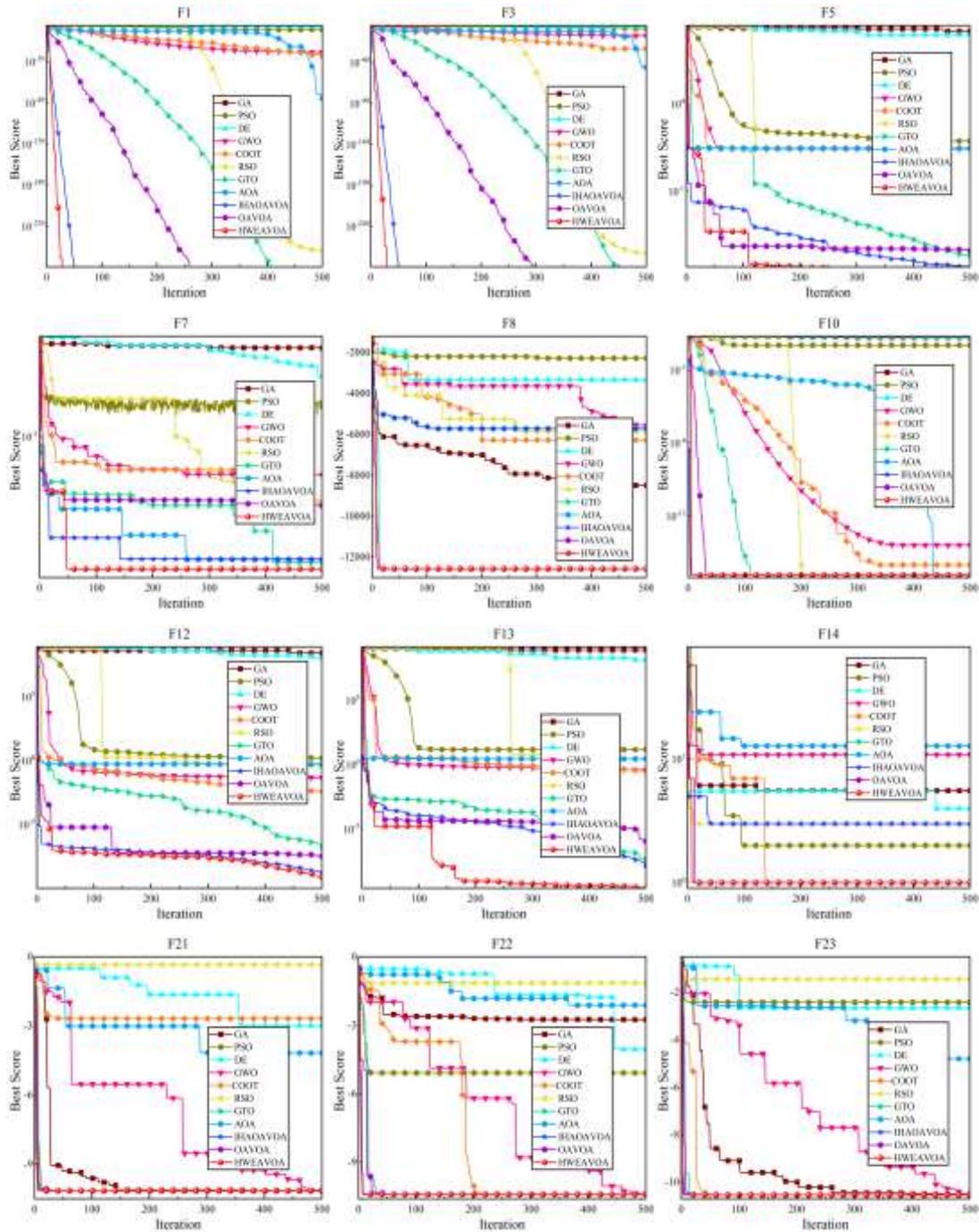


Fig. 6. Convergence curves of HWEAVOA and advanced algorithms based on F1, F3, F5, F7, F8, F10, F12, F13, F14, F21, F22 and F23.

4.4 Evaluation with the CEC2022 test functions

After using classical test functions to comprehensively evaluate the proposed HWEAVOA, the CEC2022 test functions (Dimension = 10 and 20) is applied to comprehensively evaluate the algorithm. The purpose of this section is to provide a reference for subsequent research, so that other scholars can compare and evaluate the AVOA based on the CEC2022 test functions. To be fair, all

95 algorithms are performed under the same test conditions. The parameter settings of the algorithms are
96 shown in Table 3.

97 In the CEC2022 test functions, F1 is the unimodal function, F2~F5 are basic functions, F6~F8
98 are hybrid functions, and F9~F12 are the composition functions. Different types of test functions can
99 be used to evaluate the algorithm performance from different aspects. The experimental results of the
100 HWEAVOA with 10 and 20 dimensions are shown in Table 7 and Table 8.

101 The experimental results in Table 7 and Table 8 present that the HWEAVOA can obtain the
102 competitive results consistently in almost all test functions for both 10 and 20 dimensions successfully.
103 For the whole CEC2022 test functions, the HWEAVOA's advantages are obvious, which is due that
104 the HCE strategy makes the initial population distribution more homogeneous, and enhances the
105 global optimization performance and convergence rate of the AVOA. At the same time, the RLC
106 strategy increases the diversity of the population and chance of obtaining better solutions, the bad
107 performed individuals are given learning opportunities to become dominant individuals.

108 To make the analysis more comprehensive, the Friedman test is used to compare the solution
109 results of these advanced algorithms. As shown in Table 9, the overall average ranking of HWEAVOA
110 in 10 dimension is 2.25, lower than the 2.83 of COOT and the 3.00 of OAVOA. Meanwhile, the
111 overall average ranking of HWEAVOA in 10 dimension is 2.50, far lower than the 3.75 of COOT and
112 the 4.17 of GTO. In summary, the HWEAVOA overcomes the shortcomings of the original AVOA
113 and achieves better algorithm performance with the assistance of the HCE and RLC strategy.

114 **4.5 Population size analysis**

115 In this section, the influence of the population size is examined on the classical test functions.
116 In order to adequately analyze the population size sensitivity of the HWEAVOA, the population size
117 is set respectively to 30, 60, 100 and 200 to demonstrate its influence on the HWEAVOA.

118 The experimental data are shown in Table 10, where the Avg and Std values of HWEAVOA
119 varied slightly from population size to population in 23 test functions, but the overall order of
120 magnitude remained basically at the same level. Because there is little difference between the given
121 population size, the claim as mentioned earlier is supported. Therefore, the HWEAVOA is more stable
122 when the population changes.

Table 7. The comparison results based on the CEC2022 test functions in 10 dimensions.

		GA	PSO	DE	GWO	COOT	RSO	GTO	AOA	IHAOAVOA	OAVOA	HWEAVOA
F1	Avg	1.9995E+04	3.0001E+02	-5.5927E+01	1.7534E+03	3.0000E+02	2.3436E+03	3.0000E+02	3.0001E+02	3.0000E+02	3.0000E+02	3.0000E+02
	Std	3.0080E+07	1.1900E-04	6.7143E-01	4.4890E+06	4.5500E-22	2.4512E+06	1.6200E-24	6.2700E-06	1.7200E-27	6.5719E-27	1.4100E-26
F2	Avg	6.8903E+02	4.2197E+02	5.0036E+01	4.1862E+02	4.0380E+02	5.7541E+02	4.0562E+02	4.1036E+02	4.0722E+02	4.1151E+02	4.0448E+02
	Std	1.1520E+04	9.8515E+02	7.8571E+02	3.0141E+02	1.5297E+01	2.2229E+04	1.1312E+01	5.6712E+02	1.5625E+02	4.0075E+02	1.3888E+01
F3	Avg	6.0021E+02	6.3422E+02	7.4124E+01	6.0970E+02	6.0474E+02	6.5138E+02	6.0636E+02	6.3708E+02	6.0737E+02	6.0138E+02	6.0174E+02
	Std	5.2720E-03	9.9069E+01	6.6654E+02	3.7110E+00	7.8997E+01	4.9371E+01	3.5148E+01	7.1256E+01	4.1175E+00	7.2203E-02	4.1847E+00
F4	Avg	8.3484E+02	8.4777E+02	3.4137E+01	8.1298E+02	8.3482E+02	8.3254E+02	8.3383E+02	8.2769E+02	8.3383E+02	8.3482E+02	8.2537E+02
	Std	5.3886E+01	1.1947E+02	2.8070E+02	2.8330E+01	4.8599E+01	2.2008E+01	4.7252E+01	7.5699E+01	2.7978E+01	6.2494E+01	7.6737E+01
F5	Avg	1.3542E+03	1.2216E+03	-2.5214E+01	9.5237E+02	9.0002E+02	1.1271E+03	9.7532E+02	1.2902E+03	9.4161E+02	9.0023E+02	9.0099E+02
	Std	3.1483E+04	2.6976E+04	2.0908E+00	1.1218E+02	6.8190E-03	1.4193E+04	9.0682E+03	1.0642E+04	1.1198E+04	5.1482E-02	2.9881E+00
F6	Avg	1.8176E+07	2.1505E+03	3.7966E+00	6.0399E+03	3.9331E+03	5.7324E+03	1.8094E+03	3.5362E+03	3.3599E+03	3.3628E+03	2.8883E+03
	Std	1.2712E+14	1.5391E+06	2.9026E+03	5.4581E+06	2.6374E+06	2.9482E+14	1.2809E+02	2.1892E+06	2.0490E+06	3.1717E+06	1.0477E+06
F7	Avg	2.0208E+03	2.0636E+03	1.7459E+01	2.0241E+03	2.0181E+03	2.0634E+03	2.0267E+03	2.0829E+03	2.0190E+03	2.0199E+03	2.0138E+03
	Std	8.3430E+01	5.3316E+02	9.3407E+03	1.5463E+02	4.7923E+01	4.2172E+02	1.0953E+02	4.0626E+02	3.8705E+01	2.4507E+01	8.6743E+01
F8	Avg	2.2392E+03	2.2698E+03	-1.1462E+01	2.2208E+03	2.2221E+03	2.2370E+03	2.2209E+03	2.2908E+03	2.2168E+03	2.2162E+03	2.2179E+03
	Std	2.3366E+01	3.9262E+03	4.4070E+01	4.5022E+01	6.3696E+01	6.3623E+01	1.2209E+01	7.3968E+03	6.1120E+01	6.4969E+01	4.6032E+01
F9	Avg	2.5427E+03	2.5401E+03	-1.0000E+02	2.5531E+03	2.5293E+03	2.6010E+03	2.5293E+03	2.5337E+03	2.5293E+03	2.5293E+03	2.5293E+03
	Std	5.9104E+01	1.3256E+03	8.2500E-26	8.0224E+02	0.0000E+00	2.9113E+03	0.0000E+00	5.5817E+02	0.0000E+00	4.8344E-26	0.0000E+00
F10	Avg	2.5008E+03	2.6670E+03	-3.4148E+01	2.5747E+03	2.5003E+03	2.5084E+03	2.5262E+03	2.6651E+03	2.5003E+03	2.5003E+03	2.5003E+03
	Std	4.2841E-02	5.6401E+04	5.4604E+02	2.7634E+03	3.9770E-03	1.0054E+02	2.6568E+03	1.5394E+04	4.4440E-03	9.0221E-03	8.3947E-03
F11	Avg	2.8061E+03	2.7291E+03	5.4929E+01	2.8138E+03	2.6000E+03	3.0906E+03	2.7505E+03	2.7508E+03	2.6500E+03	2.6267E+03	2.6684E+03
	Std	3.2922E+03	2.2252E+04	2.9914E+02	2.8021E+04	2.7700E-13	1.3164E+05	2.6160E+03	2.3527E+04	1.5006E+04	9.9556E+03	1.8921E+04
F12	Avg	2.8706E+03	2.9848E+03	-6.6854E+01	2.8878E+03	2.8612E+03	2.9397E+03	2.8684E+03	2.9947E+03	2.8666E+03	2.8659E+03	2.8644E+03
	Std	8.0265E+00	6.0686E+03	1.1489E+03	3.1006E+01	5.1857E+00	4.2442E+02	2.4881E+00	4.3692E+03	3.4936E+00	2.9429E+00	3.6782E+01

Table 8. The comparison results based on the CEC2022 test functions in 20 dimensions.

		GA	PSO	DE	GWO	COOT	RSO	GTO	AOA	IHAOAVOA	OAVOA	HWEAVOA
F1	Avg	7.6011E+04	7.0912E+02	8.1813E+02	6.6808E+03	3.0000E+02	1.4181E+04	3.0000E+02	3.0010E+02	3.0000E+02	3.0000E+02	3.0000E+02
	Std	2.0700E+08	1.5229E+06	2.6637E+06	1.3043E+07	3.4400E-21	3.3025E+07	1.1300E-20	5.0100E-04	5.3900E-28	9.8600E-26	1.4000E-27
F2	Avg	1.2841E+03	4.5225E+02	4.3727E+02	4.9385E+02	4.3273E+02	8.6792E+02	4.2849E+02	4.5527E+02	4.2497E+02	4.2916E+02	4.2891E+02
	Std	3.9865E+04	6.4405E+02	6.0584E+02	1.2853E+03	5.2264E+02	5.3667E+04	5.4241E+02	1.1691E+02	5.5722E+02	5.4359E+02	5.8716E+02
F3	Avg	6.0015E+02	6.5143E+02	6.0119E+02	6.0267E+02	6.0564E+02	6.6415E+02	6.3209E+02	6.5379E+02	6.0194E+02	6.0070E+02	6.0093E+02
	Std	2.9210E-03	4.3689E+01	1.2426E+00	6.8511E+00	2.4144E+01	5.5494E+01	1.4569E+02	4.2390E+01	6.9376E+00	1.1823E+00	9.3945E-01
F4	Avg	8.7881E+02	8.8546E+02	8.3256E+02	8.4287E+02	8.6192E+02	9.1696E+02	8.7668E+02	8.8276E+02	8.8832E+02	8.8245E+02	8.6169E+02
	Std	7.9420E+02	4.7240E+02	2.2830E+02	1.3756E+02	2.8356E+02	2.1794E+02	2.7295E+02	3.3106E+02	1.6662E+02	2.1975E+02	1.6810E+02
F5	Avg	2.9479E+03	2.2782E+03	9.6690E+02	1.1245E+03	1.1783E+03	2.3423E+03	1.8932E+03	2.3299E+03	2.3803E+03	2.2113E+03	2.1837E+03
	Std	5.8630E+05	2.8727E+05	8.5202E+03	3.2871E+04	4.2179E+04	6.2006E+04	1.8306E+05	7.2733E+04	2.7854E+04	8.0193E+04	7.9051E+04
F6	Avg	2.9100E+08	2.7457E+03	8.9529E+03	3.5561E+04	5.1210E+03	7.2939E+07	2.1717E+03	5.1852E+03	3.7880E+03	5.3965E+03	3.9485E+03
	Std	1.2400E+16	1.3924E+06	4.7130E+07	7.2722E+09	1.2043E+07	6.6014E+15	2.1407E+05	4.3895E+06	6.7910E+06	2.5995E+07	9.7389E+06
F7	Avg	2.0340E+03	2.1553E+03	2.0493E+03	2.0499E+03	2.0497E+03	2.1451E+03	2.0888E+03	2.2145E+03	2.0514E+03	2.0496E+03	2.0483E+03
	Std	1.4750E+02	2.4396E+03	9.1386E+02	3.2555E+02	1.7747E+02	2.2516E+02	7.2408E+02	8.5310E+03	2.7604E+02	4.2926E+02	3.4070E+02
F8	Avg	2.3153E+03	2.4193E+03	2.2310E+03	2.2324E+03	2.2224E+03	2.3537E+03	2.2290E+03	2.4171E+03	2.2224E+03	2.2241E+03	2.2211E+03
	Std	1.1899E+03	2.7272E+04	8.9604E+02	8.7208E+02	1.2782E+00	1.8685E+05	5.3493E+01	1.8651E+04	1.0029E+00	2.7518E+01	1.1947E+01
F9	Avg	2.4935E+03	2.4971E+03	2.4820E+03	2.5026E+03	2.4808E+03	2.6100E+03	2.4808E+03	2.4812E+03	2.4808E+03	2.4808E+03	2.4808E+03
	Std	7.3402E+01	1.0619E+03	1.0095E+01	3.7589E+02	8.3300E-23	2.4678E+03	3.9300E-21	7.7460E-03	3.7200E-25	1.7400E-20	4.1200E-23
F10	Avg	2.5011E+03	4.4796E+03	2.9458E+03	3.0890E+03	2.5051E+03	3.2196E+03	2.5260E+03	4.0394E+03	2.5070E+03	2.5133E+03	2.4855E+03
	Std	4.9107E-02	8.0914E+05	2.3697E+05	2.0353E+05	6.7290E+02	1.2280E+06	4.1784E+03	7.5209E+05	2.9393E+03	2.7125E+03	1.2669E+03
F11	Avg	3.7768E+03	3.3455E+03	3.0111E+03	3.5129E+03	2.9300E+03	5.5933E+03	2.9253E+03	3.4189E+03	2.9400E+03	2.9033E+03	2.9167E+03
	Std	4.8404E+04	1.2588E+06	2.7757E+04	2.3169E+05	6.1000E+03	1.2507E+06	1.5425E+04	2.2891E+06	2.4000E+03	8.3222E+03	9.3889E+03
F12	Avg	2.9770E+03	3.9106E+03	2.9807E+03	2.9639E+03	2.9595E+03	3.1601E+03	2.9750E+03	3.5943E+03	2.9581E+03	2.9528E+03	2.9571E+03
	Std	3.1631E+02	8.5495E+04	1.4352E+03	3.4093E+02	3.6502E+02	1.4400E+04	1.3039E+03	3.0793E+04	2.5189E+02	1.1766E+02	1.7181E+02

Table 9. The Friedman test results based on the CEC2022 test functions in 10 and 20 dimensions.

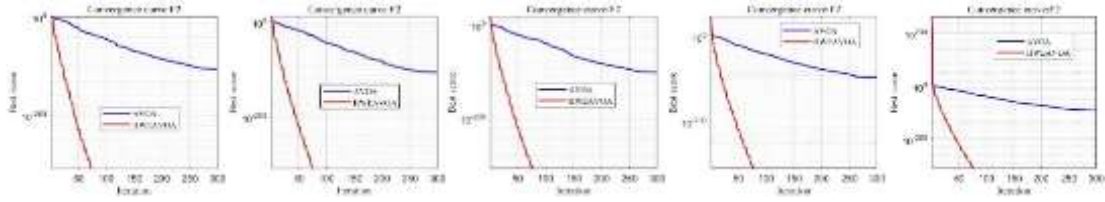
	GA	PSO	DE	GWO	COOT	RSO	GTO	AOA	IHAOAVOA	OAVOA	HWEAVOA
Dimension=10											
F1	10	6	11	8	1	9	1	6	1	1	1
F2	10	8	11	7	1	9	3	5	4	6	2
F3	1	8	11	7	4	10	5	9	6	2	3
F4	9	10	11	1	7	4	5	3	5	7	2
F5	10	8	11	6	1	7	5	9	4	2	3
F6	2	3	11	10	8	9	1	7	5	6	4
F7	5	9	11	6	2	8	7	10	3	4	1
F8	8	9	11	4	6	7	5	10	2	1	3
F9	8	7	11	9	1	10	1	6	1	1	1
F10	5	10	11	8	1	6	7	9	1	1	1
F11	8	5	11	9	1	10	6	7	3	2	4
F12	6	9	11	7	1	8	5	10	4	3	2
Avg. Rank/No.	6.83/6	7.67/9	11/11	6.83/6	2.83/2	8.08/10	4.25/5	7.58/8	3.25/4	3.00/3	2.25/1
Dimension=20											
F1	8	7	9	10	1	11	1	6	1	1	1
F2	11	7	6	9	5	10	2	8	1	4	3
F3	1	9	4	6	7	11	8	10	5	2	3
F4	6	9	1	2	4	11	5	8	10	7	3
F5	11	7	1	2	3	9	4	8	10	6	5
F6	3	2	11	4	7	10	1	8	5	9	6
F7	1	10	3	6	5	9	8	11	7	4	2
F8	8	11	6	7	2	9	5	10	2	4	1
F9	8	9	7	10	1	11	1	6	1	1	1
F10	2	11	7	8	3	9	6	10	4	5	1
F11	10	7	6	9	4	11	3	8	5	1	2
F12	7	11	8	5	4	9	6	10	3	1	2
Avg. Rank/No.	6.33/7	8.33/9	5.75/6	6.50/8	3.83/4	10.00/11	4.17/3	8.58/10	4.50/5	3.75/2	2.50/1

Table 10. Sensitivity analysis of different population sizes based on 23 classical functions.

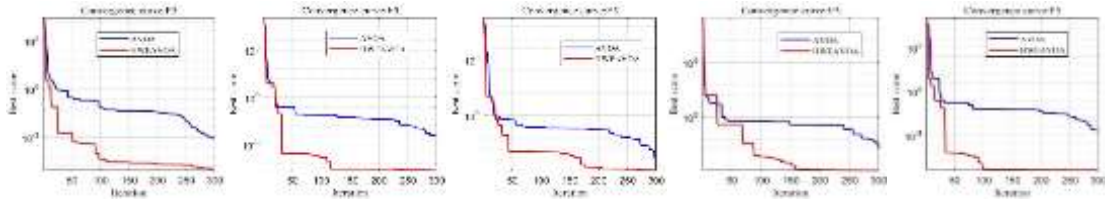
		30	60	100	200
F1	Avg	0.0000E+00	0.0000E+00	0.0000E+00	0.0000E+00
	Std	0.0000E+00	0.0000E+00	0.0000E+00	0.0000E+00
F2	Avg	0.0000E+00	0.0000E+00	0.0000E+00	0.0000E+00
	Std	0.0000E+00	0.0000E+00	0.0000E+00	0.0000E+00
F3	Avg	0.0000E+00	0.0000E+00	0.0000E+00	0.0000E+00
	Std	0.0000E+00	0.0000E+00	0.0000E+00	0.0000E+00
F4	Avg	0.0000E+00	0.0000E+00	0.0000E+00	0.0000E+00
	Std	0.0000E+00	0.0000E+00	0.0000E+00	0.0000E+00
F5	Avg	5.1640E-03	5.2367E-03	8.5621E-04	1.7253E-03
	Std	9.3618E-06	3.4359E-05	1.4911E-07	9.4956E-06
F5	Avg	5.5716E-07	1.1698E-06	1.7265E-06	1.2100E-07
	Std	7.2768E-13	1.4465E-11	3.6144E-12	2.1064E-12
F7	Avg	1.2076E-05	5.9481E-05	3.7508E-05	1.7748E-05
	Std	1.4328E-09	3.5820E-09	1.5147E-09	3.0263E-10
F8	Avg	-1.2527E+04	-1.2103E+04	-1.2204E+04	-1.2371E+04
	Std	8.6230E+03	5.5886E+03	4.2403E+04	2.8936E+03
F9	Avg	0.0000E+00	0.0000E+00	0.0000E+00	0.0000E+00
	Std	0.0000E+00	0.0000E+00	0.0000E+00	0.0000E+00
F10	Avg	8.8818E-16	8.8818E-16	8.8818E-16	8.8818E-16
	Std	0.0000E+00	0.0000E+00	0.0000E+00	0.0000E+00
F11	Avg	0.0000E+00	0.0000E+00	0.0000E+00	0.0000E+00
	Std	0.0000E+00	0.0000E+00	0.0000E+00	0.0000E+00
F12	Avg	5.7613E-09	2.5498E-07	2.5966E-08	2.6022E-08
	Std	2.5338E-15	1.5462E-11	1.9803E-14	1.8059E-15
F13	Avg	7.3758E-08	4.0968E-06	1.1280E-07	3.4556E-08
	Std	1.1564E-14	5.0752E-12	4.2136E-14	3.7311E-15
F14	Avg	1.2568E+00	1.4675E+00	1.2382E+00	1.0843E+00
	Std	4.2014E-01	6.0182E-01	3.6571E-01	1.5693E-01
F15	Avg	3.1114E-04	5.8826E-04	5.1128E-04	4.0008E-04
	Std	5.9227E-09	6.2153E-09	5.8469E-09	2.7391E-08
F16	Avg	-1.0316E+00	-1.0316E+00	-1.0316E+00	-1.0316E+00
	Std	2.0454E-28	1.4192E-26	5.0793E-31	6.2861E-30
F17	Avg	3.9789E-01	3.9789E-01	3.9789E-01	3.9789E-01
	Std	5.4939E-28	5.3416E-29	3.9154E-26	6.7903E-29
F18	Avg	3.0270E+00	3.0000E+00	3.0270E+00	3.0000E+00
	Std	7.2827E-10	8.1005E-09	3.6158E-10	1.1593E-12
F19	Avg	-3.8628E+00	-3.8628E+00	-3.8628E+00	-3.8628E+00
	Std	8.6647E-15	4.5036E-18	1.7259E-20	1.6654E-15
F20	Avg	-3.2713E+00	-3.2668E+00	-3.2623E+00	-3.2561E+00
	Std	3.5391E-03	3.5244E-03	3.5389E-03	3.4928E-03
F21	Avg	-1.0153E+01	-1.0153E+01	-1.0153E+01	-1.0153E+01
	Std	1.9212E-20	5.1396E-21	7.5399E-18	4.7699E-20
F22	Avg	-1.0402E+01	-1.0402E+01	-1.0402E+01	-1.0402E+01
	Std	5.5748E-20	1.0652E-21	1.9089E-17	3.8890E-20
F23	Avg	-1.0536E+01	-1.0536E+01	-1.0536E+01	-1.0536E+01
	Std	3.9712E-20	7.5420E-21	1.7320E-17	7.6821E-20

128 **4.6 Scalability analysis**

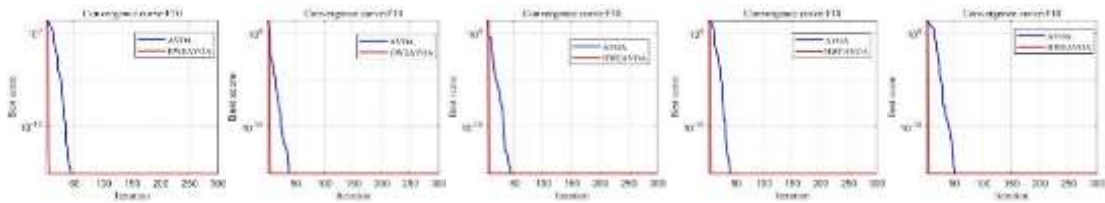
129 In this section, the scalability of the proposed HWEAVOA and AVOA is investigated using the
 130 classical test functions with different dimension sizes, including dimension = 10, 30, 50, 100, and
 131 1000. The experimental results of using thirteen classical functions (F1~F13) with different
 132 dimensions sizes is shown in Table 11.



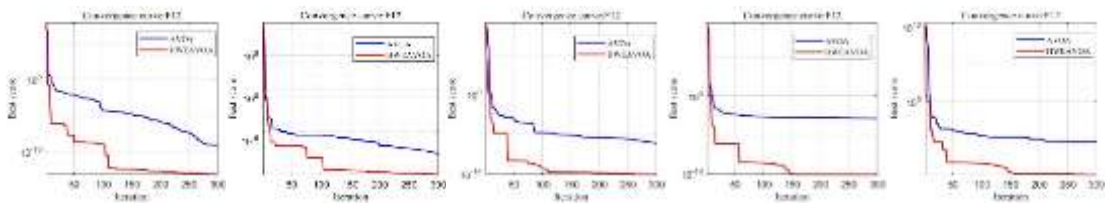
133 (1) the F2, dimension =10,30,50,100,1000



134 (2) the F5, dimension =10,30,50,100,1000



135 (3) the F10, dimension =10,30,50,100,1000



136 (4) the F12, dimension =10,30,50,100,1000

137 Fig. 7. Convergence curves of HWEAVOA and AVOA based on F2, F5, F10, F12 in different dimensions.

142 When solving functions F1~F4, F9, F10 and F11, the optimal values in five different function
 143 dimensions can be obtained by HWEAVOA. Although the optimal values of other functions in
 144 different dimensions cannot be obtained, the searchability and algorithm stability of HWEAVOA are
 145 still better than AVOA. As shown in Fig. 7, the HWEAVOA algorithm dramatically improves the
 146 convergence speed and solving accuracy in the solution space when dealing with problems in different

Table 11. Effects of different dimensions on HWEAVOA and AVOA.

F1	Avg		Std		F2	Avg		Std	
	HWEAVOA	AVOA	HWEAVOA	AVOA		HWEAVOA	AVOA	HWEAVOA	AVOA
10	0.0000E+00	7.4754E-156	0.0000E+00	4.1317E-308	10	0.0000E+00	3.8718E-85	0.0000E+00	9.6229E-167
30	0.0000E+00	1.8798E-152	0.0000E+00	3.4069E-301	30	0.0000E+00	5.5067E-79	0.0000E+00	2.9615E-154
50	0.0000E+00	2.5469E-155	0.0000E+00	4.8062E-307	50	0.0000E+00	2.8717E-80	0.0000E+00	8.0247E-157
100	0.0000E+00	7.5766E-155	0.0000E+00	5.2743E-306	100	0.0000E+00	7.7134E-76	0.0000E+00	5.9317E-148
1000	0.0000E+00	2.4051E-142	0.0000E+00	5.7688E-281	1000	0.0000E+00	3.7049E-89	0.0000E+00	1.1958E-174
F3	Avg		Std		F4	Avg		Std	
	HWEAVOA	AVOA	HWEAVOA	AVOA		HWEAVOA	AVOA	HWEAVOA	AVOA
10	0.0000E+00	6.6029E-126	0.0000E+00	4.3427E-248	10	0.0000E+00	8.3521E-82	0.0000E+00	3.5317E-160
30	0.0000E+00	6.8769E-109	0.0000E+00	4.6984E-214	30	0.0000E+00	8.8211E-77	0.0000E+00	6.4879E-150
50	0.0000E+00	2.4443E-99	0.0000E+00	5.9264E-195	50	0.0000E+00	4.8276E-78	0.0000E+00	1.3497E-152
100	0.0000E+00	4.8091E-86	0.0000E+00	2.3068E-168	100	0.0000E+00	3.5643E-76	0.0000E+00	1.2583E-148
1000	0.0000E+00	2.7765E-24	0.0000E+00	7.6591E-45	1000	0.0000E+00	3.7161E-78	0.0000E+00	1.3528E-152
F5	Avg		Std		F6	Avg		Std	
	HWEAVOA	AVOA	HWEAVOA	AVOA		HWEAVOA	AVOA	HWEAVOA	AVOA
10	1.5708E-01	1.0491E+00	5.6701E-01	3.2174E+00	10	1.1328E-09	1.7057E-05	2.1213E-18	2.6187E-07
30	8.3167E-02	1.6046E-01	2.2622E+00	4.2509E+00	30	2.5976E-04	1.2587E-03	4.2497E-06	3.0561E-04
50	4.7133E-02	2.1518E+00	9.5856E-02	4.4630E+00	50	1.5179E-03	3.2196E-04	2.0168E-03	4.6227E-04
100	2.5488E-03	1.1534E-05	3.8857E-03	3.6376E-04	100	4.8263E-03	2.2146E-02	1.2379E-03	6.1494E-03
1000	5.6482E-02	2.2465E-01	5.6786E-02	1.5965E+01	1000	6.9354E-02	4.9993E-01	2.6118E-01	1.0005E+00
F7	Avg		Std		F8	Avg		Std	
	HWEAVOA	AVOA	HWEAVOA	AVOA		HWEAVOA	AVOA	HWEAVOA	AVOA
10	1.1536E-04	2.7483E-04	1.2103E-08	8.9476E-08	10	-3.9239E+03	-3.8095E+05	1.6718E+05	2.6001E+05
30	1.1475E-04	2.8733E-04	1.1029E-08	9.6857E-08	30	-1.2225E+04	-1.2001E+04	3.8323E+05	7.7594E+05

50	1.2269E-04	2.7314E-04	1.5506E-08	8.6481E-08	50	-2.0366E+04	-1.9818E+04	9.7411E+05	2.4067E+06
100	1.1728E-04	2.8791E-04	1.4503E-08	9.6452E-08	100	-4.0630E+04	-3.8769E+04	4.1081E+06	1.3336E+07
1000	1.2293E-04	3.2956E-04	1.3847E-08	1.2399E-07	1000	-4.0110E+05	-3.8088E+05	5.5598E+08	1.8369E+09
F9	Avg		Std		F10	Avg		Std	
	HWEAVOA	AVOA	HWEAVOA	AVOA		HWEAVOA	AVOA	HWEAVOA	AVOA
10	0.0000E+00	0.0000E+00	0.0000E+00	0.0000E+00	10	8.8818E-16	8.8818E-16	0.0000E+00	0.0000E+00
30	0.0000E+00	0.0000E+00	0.0000E+00	0.0000E+00	30	8.8818E-16	8.8818E-16	0.0000E+00	0.0000E+00
50	0.0000E+00	0.0000E+00	0.0000E+00	0.0000E+00	50	8.8818E-16	8.8818E-16	0.0000E+00	0.0000E+00
100	0.0000E+00	0.0000E+00	0.0000E+00	0.0000E+00	100	8.8818E-16	8.8818E-16	0.0000E+00	0.0000E+00
1000	0.0000E+00	0.0000E+00	0.0000E+00	0.0000E+00	1000	8.8818E-16	8.8818E-16	0.0000E+00	0.0000E+00
F11	Avg		Std		F12	Avg		Std	
	HWEAVOA	AVOA	HWEAVOA	AVOA		HWEAVOA	AVOA	HWEAVOA	AVOA
10	0.0000E+00	0.0000E+00	0.0000E+00	0.0000E+00	10	1.9726E-09	1.1453E-04	1.6187E-17	1.8564E-06
30	0.0000E+00	0.0000E+00	0.0000E+00	0.0000E+00	30	4.4074E-05	5.4329E-05	1.6852E-07	5.4209E-07
50	0.0000E+00	0.0000E+00	0.0000E+00	0.0000E+00	50	5.9236E-05	8.2077E-05	1.8501E-07	4.2768E-07
100	0.0000E+00	0.0000E+00	0.0000E+00	0.0000E+00	100	4.5862E-05	1.1193E-04	7.3659E-08	3.2847E-07
1000	0.0000E+00	0.0000E+00	0.0000E+00	0.0000E+00	1000	1.8633E-05	8.8364E-05	2.0078E-08	8.0957E-08
F13	Avg		Std						
	HWEAVOA	AVOA	HWEAVOA	AVOA					
10	1.1078E-05	1.4781E-04	1.2179E-07	1.2153E-05					
30	1.2236E-04	4.3281E-04	1.0019E-05	2.6475E-05					
50	2.3369E-04	2.7411E-04	1.3704E-05	2.0068E-05					
100	7.9216E-04	8.9577E-04	1.8364E-04	3.2531E-04					
1000	4.8569E-03	2.2227E-02	2.8346E-03	2.4359E-02					

149 dimensions compared with the original AVOA. Meanwhile, as shown in Table 6 and Table 7, the
 150 HWEAVOA all takes the leading positions in the top three when solving CEC2022 test functions
 151 F1~F4, F7~F10 and F12. The above analysis shows that HWEAVOA has a better ability to deal with
 152 high-dimensional problems than that of the original AVOA.

153 4.7 Time consumption and algorithm complexity analysis

154 In order to study the time consumption of HWEAVOA, the running time of HWEAVOA and
 155 other advanced algorithms in classical test functions is shown in the Table 12, where the unit of
 156 measurement is seconds.

157 Experimental results show the time consumption of HWEAVOA is similar to that of the original
 158 AVOA and inferior compared to some classical optimization algorithms, but the algorithm accuracy
 159 and stability of HWEAVOA is leading. These experimental results demonstrate that the overall search
 160 performance of HWEAVOA has not been affected. Therefore, HWEAVOA has higher search
 161 efficiency than other advanced algorithms.

162 Table 12. Time consumption (measured in seconds) of different algorithms.

	AVOA	GA	PSO	DE	GWO	COOT	RSO	GTO	AOA	IHAOAVOA	OAVOA	HWEAVOA
F1	0.0702	0.0347	0.0351	0.0029	0.1020	0.0353	0.0550	0.1174	0.0511	0.1316	0.1529	0.1061
F2	0.0724	0.0351	0.0329	0.0029	0.0965	0.0370	0.0514	0.1229	0.0516	0.1345	0.1576	0.1126
F3	0.1629	0.1213	0.2822	0.0049	0.1811	0.1183	0.1928	0.2837	0.1365	0.4085	0.3171	0.3728
F4	0.0697	0.0334	0.0331	0.0028	0.0945	0.0355	0.0516	0.1172	0.0498	0.1255	0.1537	0.1025
F5	0.0814	0.0425	0.0526	0.0031	0.1056	0.0453	0.0712	0.1412	0.0628	0.1631	0.1728	0.1345
F6	0.0725	0.0333	0.0366	0.0028	0.0944	0.0360	0.0503	0.1180	0.0506	0.1261	0.1537	0.1022
F7	0.1122	0.0706	0.1136	0.0041	0.1340	0.0793	0.1163	0.2000	0.0877	0.2398	0.2244	0.2177
F8	0.0860	0.0437	0.0559	0.0031	0.1139	0.0483	0.0727	0.1393	0.0625	0.1565	0.1798	0.1245
F9	0.0765	0.0404	0.0432	0.0031	0.0958	0.0418	0.0615	0.1211	0.0506	0.1308	0.1628	0.1038
F10	0.0737	0.0388	0.0467	0.0031	0.0909	0.0399	0.0609	0.1135	0.0503	0.1223	0.1422	0.1029
F11	0.0843	0.0496	0.0868	0.0033	0.1041	0.0511	0.0739	0.1370	0.0630	0.1591	0.1828	0.1304
F12	0.1838	0.1509	0.3400	0.0061	0.2120	0.1533	0.2506	0.3218	0.1547	0.4169	0.4394	0.3328
F13	0.1918	0.1505	0.3436	0.0060	0.2154	0.1545	0.2425	0.3390	0.1488	0.4317	0.4365	0.3406
F14	0.2851	0.2215	0.4634	0.0069	0.2207	0.2173	0.4285	0.4383	0.1901	0.5863	0.7902	0.4102
F15	0.0498	0.0180	0.0266	0.0011	0.0277	0.0287	0.0322	0.0820	0.0228	0.0985	0.1115	0.0786
F16	0.0504	0.0165	0.0241	0.0009	0.0216	0.0270	0.0301	0.0790	0.0197	0.0917	0.1088	0.0755
F17	0.0453	0.0191	0.0258	0.0009	0.0208	0.0291	0.1496	0.0799	0.0213	0.0955	0.1099	0.0693
F18	0.0467	0.0129	0.0170	0.0008	0.0185	0.0245	0.0226	0.0743	0.0160	0.0790	0.0984	0.0635
F19	0.0439	0.0177	0.0274	0.0011	0.0244	0.0268	0.0370	0.0752	0.0208	0.0851	0.0940	0.0750
F20	0.0385	0.0161	0.0241	0.0013	0.0256	0.0227	0.0391	0.0645	0.0201	0.0755	0.0861	0.0633
F21	0.0418	0.0193	0.0331	0.0014	0.026	0.0272	0.0462	0.0718	0.0230	0.0875	0.0936	0.0753
F22	0.0550	0.0296	0.0510	0.0015	0.0370	0.0388	0.0558	0.1001	0.0322	0.1230	0.1283	0.1092
F23	0.0756	0.0404	0.0719	0.0017	0.0475	0.0493	0.0685	0.1210	0.0421	0.1576	0.1473	0.1539

163 Moreover, the algorithm complexity is also an important evaluation basis for optimization
 164 algorithms. Therefore, the algorithm complexity is calculated based on the CEC2022 test functions.
 165 According to the Literature (Sun, Sun, Li, & Ieee, 2022), the calculation rules are as follows:

166 (1) Run the test program below:

```

167     x = 0.55
168     for i = 1: 200000
169         x = x + x; x = x / 2; x = x * x, x = sqrt(x);
170         x = log(x); x = exp(x); x = x / (x + 2);
171     end
  
```

172 (2) Evaluate the time consumption for CEC2022 test function F1 with 200,000 evaluations of a
 173 certain dimension D , it is $T1$;

174 (3) Evaluate the complete time for the mentioned algorithms with 200,000 evaluations of the
 175 same D dimensional F1, it is $T2$;

176 (4) Calculate $T2$ for 5 independent runs, $T2 = mean(T2)$.

177 Finally, the algorithm complexity is calculated as $(T2 - T1) / T0$. According to the above method,
 178 the algorithm complexity for HWEAVOA and other improved algorithms is shown in Table 13.

179 Table 13. The algorithm complexity of the HWEAVOA and other advanced algorithms.

Dimension	AVOA	GA	PSO	DE	GWO	COOT	RSO	GTO	AOA	IHAOAVOA	OAVOA	HWEAVOA
10	72.83	45.81	82.86	2.29	60.98	54.50	58.49	132.43	54.34	193.54	163.92	74.24
20	72.70	47.30	80.51	2.37	71.00	53.48	59.12	134.24	57.68	190.63	171.96	73.54

180 Table 13 indicates that the HWEAVOA lost to part of the advanced algorithms for the algorithm
 181 complexity when Dimension = 10 and 20. However, HWEAVOA can achieve relatively competitive
 182 results with very small iterations throughout the convergence process, which lead other algorithms in
 183 the overall performance. On the whole, combined with the previous researches (Sun, Li, Huang, &
 184 Ieee, 2022), the result of the HWEAVOA has reached the general level of swarm intelligence
 185 algorithms and it is also competitive in the algorithm complexity.

186 4.8 Wilcoxon rank sum test

187 Although the test results of classical and CEC2022 test functions show the superiority of
 188 HWEAVOA in some extent, due to the stochastic nature of meta-heuristic algorithms, it is important

Table 14. *p*-Value for Wilcoxon rank and test results based on the CEC2022 test functions in 10 and 20 dimensions.

	AVOA <i>p</i> -value win	GA <i>p</i> -value win	PSO <i>p</i> -value win	DE <i>p</i> -value win	GWO <i>p</i> -value win	COOT <i>p</i> -value win	RSO <i>p</i> -value win	GTO <i>p</i> -value win	AOA <i>p</i> -value win	IHAOAVOA <i>p</i> -value win	OAVOA <i>p</i> -value win
Dimension=10											
F1	6.5183E-09 =	2.8719E-11 +	2.8719E-11 +	1.0666E-07+	2.8719E-11 +	2.8719E-11 =	2.8719E-11 +	7.9782E-02 =	2.8719E-11 +	2.1284E-09 =	1.2685E-03 =
F2	3.1830E-01 +	2.8719E-11 +	2.8663E-02 +	5.5611E-04+	4.2666E-06 +	7.0069E-01 -	2.8719E-11 +	6.0484E-01 +	1.0707E-01 +	3.6322E-01 +	8.7663E-01 +
F3	6.8023E-08 +	1.9494E-02 -	2.8719E-11 +	1.3825E-05+	2.5495E-01 +	8.7945E-04 +	2.8719E-11 +	8.5825E-06 +	2.8719E-11 +	1.2470E-02 +	1.4787E-05 -
F4	1.2597E-01 +	4.7792E-01 +	5.3464E-01 +	5.5727E-10+	5.8188E-07 -	4.7885E-05 +	6.0361E-04 +	1.6461E-01 +	3.2918E-01 +	1.5798E-01 +	6.8432E-01 +
F5	3.3681E-05 -	1.7938E-06 +	1.0727E-04 +	3.3258E-02+	3.2054E-02 +	1.3690E-08 -	2.6046E-04 +	3.3258E-02 +	4.7885E-05 +	8.8247E-01 +	4.4205E-06 -
F6	6.6763E-02 +	2.8719E-11 -	1.1513E-08 -	3.0566E-05+	3.9739E-06 +	9.6739E-03 +	1.2556E-08 +	2.8719E-11 -	6.8990E-02 +	9.5284E-01 +	9.4107E-01 +
F7	1.1284E-05 +	5.7668E-08 +	3.8787E-11 +	1.4119E-02+	4.1614E-01 +	1.3549E-02 +	2.8719E-11 +	6.5216E-03 +	2.8719E-11 +	1.4493E-04 +	1.9494E-02 +
F8	9.5284E-01 +	2.8719E-11 +	5.7730E-11 +	3.0071E-01+	1.0856E-03 +	1.3549E-02 +	2.8719E-11 +	4.7454E-03 +	2.8719E-11 +	3.9117E-01 -	2.8047E-01 -
F9	1.2658E-10 =	2.8719E-11 +	1.2658E-10 +	3.9395E-03+	2.8719E-11 +	2.8719E-11 =	3.9998E-09 +	2.8719E-11 =	2.8719E-11 +	2.8719E-11 =	8.2450E-01 =
F10	3.3656E-01 +	1.4376E-06 +	3.0561E-09 +	1.4787E-05+	1.0097E-02 +	1.2044E-07 =	1.0670E-06 +	1.4796E-03 +	5.3167E-10 +	3.5783E-02 =	1.1959E-02 =
F11	1.1467E-02 +	7.8929E-07 +	1.2077E-05 +	7.7863E-03+	3.7006E-06 +	3.8778E-04 -	1.6266E-08 +	2.1105E-07 +	9.1932E-06 +	9.1809E-07 -	1.0856E-03 -
F12	9.3341E-02 +	8.1211E-09 +	3.8787E-11 +	3.9881E-04+	1.6016E-01 +	7.7863E-03 -	2.7927E-09 +	8.3026E-01 +	2.8719E-11 +	5.4441E-01 +	2.4625E-02 +
+/-/-	9/2/1	10/0/2	11/0/1	12/0/0	11/0/1	5/3/4	12/0/0	9/2/1	12/0/0	7/3/2	5/3/4
Dimension=20											
F1	8.1014E-10 +	2.8719E-11 +	2.8719E-11 +	2.8719E-11 +	2.8719E-11 +	2.8719E-11 =	2.8719E-11 +	7.2208E-06 =	2.8719E-11 +	2.6099E-10 =	5.2650E-05 =
F2	1.6238E-01 +	2.8719E-11 +	1.0541E-05 +	5.7460E-02 +	6.4146E-10 +	1.9494E-02 +	2.8719E-11 +	7.3383E-05 -	2.4879E-10 +	3.6709E-03 -	5.2014E-04 +
F3	9.1809E-07 -	4.2855E-11 +	2.8719E-11 +	4.9149E-06 +	2.9757E-02 +	3.5164E-01 +	2.8719E-11 +	3.8787E-11 +	2.8719E-11 +	2.7587E-04 +	5.3081E-08 -
F4	6.1520E-02 +	8.9092E-02 +	3.6714E-01 -	1.3950E-10 -	3.5098E-11 +	2.4726E-07 +	1.7739E-09 +	4.7454E-03 +	2.3691E-01 +	4.3764E-01 +	1.5367E-01 +
F5	5.4441E-04 +	6.5575E-05 +	4.1614E-01 -	2.8719E-11 -	2.8719E-11 -	3.8787E-11 +	9.2932E-10 -	7.4937E-04 +	9.7641E-01 +	7.3628E-02 +	2.5495E-01 +
F6	3.3614E-01 -	2.8719E-11 -	7.8991E-05 +	7.3628E-02 -	5.4441E-10 +	9.1757E-03 +	2.8719E-11 +	8.0170E-08 -	1.7378E-01 +	5.4609E-02 -	3.6714E-01 +
F7	4.8713E-01 -	1.2046E-03 +	7.0436E-10 +	2.6750E-01 +	3.9117E-01 +	1.7800E-07 +	5.3167E-10 +	2.3542E-05 +	1.5370E-10 +	2.8719E-11 +	3.1752E-11 +
F8	2.8711E-01 +	2.8719E-11 +	5.2283E-11 +	2.8711E-01 +	1.0727E-04 +	4.2820E-02 +	5.2283E-11 +	1.6906E-05 +	5.2283E-11 +	2.2798E-02 +	1.5581E-01 +
F9	3.1752E-11 +	2.8719E-11 +	2.8719E-11 +	2.8719E-11 +	2.8719E-11 +	2.3768E-07 =	2.8719E-11 +	2.2539E-01 =	2.8719E-11 +	3.1752E-11 =	2.8719E-11 =
F10	1.8824E-01 +	1.0241E-07 +	5.2283E-11 +	9.3135E-10 +	7.7326E-10 +	1.5581E-01 +	3.5098E-11 +	1.4153E-07 +	1.2658E-10 +	3.5933E-01 +	8.5918E-04 +
F11	1.1436E-03 +	2.8719E-11 +	2.5138E-05 +	3.6658E-04 +	8.5630E-11 +	6.3735E-04 +	2.8719E-11 +	1.6378E-03 +	7.1014E-04 +	5.9613E-03 +	5.4336E-05 -
F12	3.5164E-01 +	3.9395E-03 +	2.8719E-11 +	6.8990E-02 +	1.5323E-02 +	7.8519E-02 +	2.8719E-11 +	8.3602E-03 +	2.8719E-11 +	8.3670E-02 +	2.2106E-03 -
+/-/-	9/0/3	11/0/1	10/0/2	9/0/3	11/0/1	10/2/0	11/0/1	8/2/2	12/0/0	8/2/2	7/2/3

191 to further illustrate the significant difference among these algorithms in the statistical way. The
192 Wilcoxon rank sum test (Manalo, Biermann, Patil, & Mehta, 2022) can be counted the significant
193 differences between algorithms, which is often used to evaluate the optimization performance of
194 improved algorithms. Therefore, the Wilcoxon rank sum test is used on the CEC2022 test functions
195 in 10 and 20 dimensions to further verify HWEAVOA at the level of α less than 0.05.

196 The statistical results of the Wilcoxon rank sum test of the HWEAVOA relative to each
197 comparison algorithm are shown in Table 14, which “+”, “=” and “-” is used to respectively indicate
198 that HWEAVOA is superior or uniform or worse than the comparison algorithms. The p -value less
199 than 0.05 indicates that HWEAVOA shows a more significant difference than the compared algorithm.

200 According to the test results in Table 13, compared with other advanced algorithms, the
201 HWEAVOA’s test p -values are all less than 0.05, and most symbols are “+”. Therefore, HWEAVOA
202 is statistically superior to other advanced algorithms, and there are significant differences between
203 HWEAVOA and these algorithms.

204 **5. Conclusions and future works**

205 To address the issues of the original AVOA (i.e., the tendency to fall into local optimum and
206 unbalance of global search stage and local search stage), an improved African vultures optimization
207 algorithm (HWEAVOA) is proposed with three efficient optimization strategies. Firstly, the Henon
208 chaotic mapping theory and elite population strategy are proposed, which improve the vulture initial
209 population's randomness and diversity; Furthermore, the nonlinear adaptive incremental inertial
210 weight factor is introduced in the location update phase, which satisfies the requirement for the
211 exploration and exploitation ability in different phases, and avoid the algorithm falling into a local
212 optimum; The addition of the reverse learning competition strategy allows the algorithm to expand
213 the discovery fields for the optimal solution, accelerate the convergence speed of the algorithm and
214 strengthen the ability to jump out of the local optimal solution. In terms of simulation test,
215 HWEAVOA and other advanced comparison algorithms are used to solve classical and CEC2022 test
216 functions. Through the comparative analysis of experimental results and convergence curves, it is
217 proved that the optimization ability and convergence speed of the HWEAVOA for solving complex
218 functions are obviously better than the other advanced algorithms. Meanwhile, HWEAVOA has

219 reached the general level in the algorithm complexity, and its overall performance is competitive in
220 the swarm intelligence algorithms.

221 The future possible works are as follows:

222 Although the proposed HWEAVOA improves the algorithm performance in the optimization
223 ability, convergence speed and solution stability, it found that the HWEAVOA also has the room for
224 improvement in time consumption and algorithmic complexity according to the argument in the
225 article. Follow-up work will be further optimized the HWEAVOA algorithm for this issue.
226 Furthermore, large-scale problems and dynamic problems are the current development trend of the
227 swarm intelligence, but many algorithms perform poorly and are prone to local optimization when
228 solving these problems. We will continue to study on the base of the HWEAVOA, and improve the
229 applicated space of swarm intelligent algorithms.

230 **CRedit authorship contribution statement**

231 **Baiyi Wang:** Conceptualization, Methodology, Analysis, Data Curation, Writing - review &
232 editing, Funding acquisition. **Zipeng Zhang:** Methodology, Supervision, Data collection, Writing –
233 original draft. **Patrick Siarry:** Investigation, Data collection, Writing – review & editing. **Xinhua**
234 **Liu:** Supervision, Funding acquisition. **Grzegorz Królczyk:** Analysis, Writing – review & editing.
235 **Dezheng Hua:** Analysis, Writing - Review & Editing. **Frantisek Brumercik:** Data collection,
236 Visualization. **Zhixiong Li:** Investigation, Project administration, Writing - review & editing.

237 **Declaration of Competing Interest**

238 The authors declare that they have no known competing financial interests or personal
239 relationships that could have appeared to influence the work reported in this paper.

240 **Data Availability**

241 All data that produce the results in this work can be requested from the corresponding author.

242 **Acknowledgements**

243 The support of National Natural Science Foundation of China (No. 51975568), the Independent
244 Innovation Project of “Double-First Class” Construction of China University of Mining and
245 Technology (2022ZZCX06) and Postgraduate Research & Practice Innovation Program of Jiangsu
246 Province (KYCX23_2681) in carrying out this research are gratefully acknowledged.

247 **References**

- 248 Abdollahzadeh, B., Gharehchopogh, F. S., & Mirjalili, S. (2021). African vultures optimization algorithm: A new
249 nature-inspired metaheuristic algorithm for global optimization problems. *Computers & Industrial*
250 *Engineering*, 158, 37.
- 251 Abualigah, L., Abd Elaziz, M., Sumari, P., Geem, Z. W., & Gandomi, A. H. (2022). Reptile Search Algorithm (RSA):
252 A nature-inspired meta-heuristic optimizer. *Expert Systems with Applications*, 191, 33.
- 253 Abualigah, L., Diabat, A., Mirjalili, S., Abd Elaziz, M., & Gandomi, A. H. (2021). The Arithmetic Optimization
254 Algorithm. *Computer Methods in Applied Mechanics and Engineering*, 376, 38.
- 255 Ahmadianfar, I., Heidari, A. A., Gandomi, A. H., Chu, X. F., & Chen, H. L. (2021). RUN beyond the metaphor: An
256 efficient optimization algorithm based on Runge Kutta method. *Expert Systems with Applications*, 181, 22.
- 257 Braik, M., Sheta, A., & Al-Hiary, H. (2021). A novel meta-heuristic search algorithm for solving optimization
258 problems: capuchin search algorithm. *Neural Computing & Applications*, 33, 2515-2547.
- 259 Cheng, R., & Jin, Y. C. (2015). A social learning particle swarm optimization algorithm for scalable optimization.
260 *Information Sciences*, 291, 43-60.
- 261 Cui, Y. F., Geng, Z. Q., Zhu, Q. X., & Han, Y. M. (2017). Review: Multi-objective optimization methods and
262 application in energy saving. *Energy*, 125, 681-704.
- 263 Das, S., & Suganthan, P. N. (2011). Differential Evolution: A Survey of the State-of-the-Art. *Ieee Transactions on*
264 *Evolutionary Computation*, 15, 4-31.
- 265 Deng, W., Li, Z. X., Li, X. Y., Chen, H. Y., & Zhao, H. M. (2022). Compound Fault Diagnosis Using Optimized
266 MCKD and Sparse Representation for Rolling Bearings. *Ieee Transactions on Instrumentation and*
267 *Measurement*, 71, 9.
- 268 Deng, W., Zhang, X. X., Zhou, Y. Q., Liu, Y., Zhou, X. B., Chen, H. L., & Zhao, H. M. (2022). An enhanced fast
269 non-dominated solution sorting genetic algorithm for multi-objective problems. *Information Sciences*, 585,
270 441-453.
- 271 Dhiman, G., Garg, M., Nagar, A., Kumar, V., & Dehghani, M. (2021). A novel algorithm for global optimization:
272 Rat Swarm Optimizer. *Journal of Ambient Intelligence and Humanized Computing*, 12, 8457-8482.
- 273 Diab, A. A. Z., Tolba, M. A., El-Rifaie, A. M., & Denis, K. A. (2022). Photovoltaic parameter estimation using
274 honey badger algorithm and African vulture optimization algorithm. *Energy Reports*, 8, 384-393.

- 275 Fan, J. H., Li, Y., & Wang, T. (2021). An improved African vultures optimization algorithm based on tent chaotic
276 mapping and time-varying mechanism. *Plos One*, *16*, 52.
- 277 Hamza, M. F., Yap, H. J., & Choudhury, I. A. (2017). Recent advances on the use of meta-heuristic optimization
278 algorithms to optimize the type-2 fuzzy logic systems in intelligent control. *Neural Computing & Applications*,
279 *28*, 979-999.
- 280 Hashim, F. A., Houssein, E. H., Hussain, K., Mabrouk, M. S., & Al-Atabany, W. (2022). Honey Badger Algorithm:
281 New metaheuristic algorithm for solving optimization problems. *Mathematics and Computers in Simulation*,
282 *192*, 84-110.
- 283 Jena, B., Naik, M. K., Panda, R., & Abraham, A. (2022). A novel minimum generalized cross entropy-based
284 multilevel segmentation technique for the brain MRI/dermoscopic images. *Computers in Biology and Medicine*,
285 *151*, 36.
- 286 Kalinli, A., & Karaboga, N. (2005). A new method for adaptive IIR filter design based on tabu search algorithm.
287 *Aeu-International Journal of Electronics and Communications*, *59*, 111-117.
- 288 Kannan, S. N., Mannathazhathu, S. E., & Raghavan, R. (2022). A novel compression based community detection
289 approach using hybrid honey badger African vulture optimization for online social networks. *Concurrency and*
290 *Computation-Practice & Experience*, *34*, 17.
- 291 Kar, A. K. (2016). Bio inspired computing - A review of algorithms and scope of applications. *Expert Systems with*
292 *Applications*, *59*, 20-32.
- 293 Karaboga, D., & Akay, B. (2009). A survey: algorithms simulating bee swarm intelligence. *Artificial Intelligence*
294 *Review*, *31*, 61-85.
- 295 Karaboga, N. (2009). A new design method based on artificial bee colony algorithm for digital IIR filters. *Journal*
296 *of the Franklin Institute-Engineering and Applied Mathematics*, *346*, 328-348.
- 297 Karaboga, N., & Cetinkaya, M. B. (2011). A novel and efficient algorithm for adaptive filtering: Artificial bee colony
298 algorithm. *Turkish Journal of Electrical Engineering and Computer Sciences*, *19*, 175-190.
- 299 Li, W., Wang, G. G., & Gandomi, A. H. (2021). A Survey of Learning-Based Intelligent Optimization Algorithms.
300 *Archives of Computational Methods in Engineering*, *28*, 3781-3799.
- 301 Liu, R. J., Wang, T. L., Zhou, J., Hao, X. X., Xu, Y., & Qiu, J. Z. (2022). Improved African Vulture Optimization
302 Algorithm Based on Quasi-Operational Differential Evolution Operator. *Ieee Access*, *10*, 95197-95218.

- 303 Manalo, T. A., Biermann, H. D., Patil, D. H., & Mehta, A. (2022). The Temporal Association of Depression and
304 Anxiety in Young Men With Erectile Dysfunction. *Journal of Sexual Medicine*, 19, 201-206.
- 305 Mekala, K., Sumathi, S., & Shobana, S. (2022). A Multi-Aggregator Based Charge Scheduling in Internet of Electric
306 Vehicles Using Fractional African Vulture Sail Fish Optimization. *Cybernetics and Systems*, 27.
- 307 Meng, O. K., Pauline, O., & Kiong, S. C. (2021). A carnivorous plant algorithm for solving global optimization
308 problems. *Applied Soft Computing*, 98, 40.
- 309 Mirjalili, S., Mirjalili, S. M., & Lewis, A. (2014). Grey Wolf Optimizer. *Advances in Engineering Software*, 69, 46-
310 61.
- 311 Nabaei, A., Hamian, M., Parsaei, M. R., Safdari, R., Samad-Soltani, T., Zarrabi, H., & Ghassemi, A. (2018).
312 Topologies and performance of intelligent algorithms: a comprehensive review. *Artificial Intelligence Review*,
313 49, 79-103.
- 314 Naruei, I., & Keynia, F. (2021). A new optimization method based on COOT bird natural life model. *Expert Systems*
315 *with Applications*, 183, 25.
- 316 Naruei, I., & Keynia, F. (2022). Wild horse optimizer: a new meta-heuristic algorithm for solving engineering
317 optimization problems. *Engineering with Computers*, 38, 3025-3056.
- 318 Oyelade, O. N., Ezugwu, A. E. S., Mohamed, T. I. A., & Abualigah, L. (2022). Ebola Optimization Search Algorithm:
319 A New Nature-Inspired Metaheuristic Optimization Algorithm. *Ieee Access*, 10, 16150-16177.
- 320 Peraza-Vazquez, H., Pena-Delgado, A., Ranjan, P., Barde, C., Choubey, A., & Morales-Cepeda, A. B. (2022). A Bio-
321 Inspired Method for Mathematical Optimization Inspired by Arachnida Salticidae. *Mathematics*, 10, 32.
- 322 Salah, B., Hasanien, H. M., Ghali, F. M. A., Alsayed, Y. M., Aleem, S., & El-Shahat, A. (2022). African Vulture
323 Optimization-Based Optimal Control Strategy for Voltage Control of Islanded DC Microgrids. *Sustainability*,
324 14, 26.
- 325 Singh, N., Houssein, E. H., Mirjalili, S., Cao, Y. K., & Selvachandran, G. (2022). An efficient improved African
326 vultures optimization algorithm with dimension learning hunting for traveling salesman and large-scale
327 optimization applications. *International Journal of Intelligent Systems*, 37, 12367-12421.
- 328 Soliman, M. A., Hasanien, H. M., Turkey, R. A., & Muyeen, S. M. (2022). Hybrid African vultures-grey wolf
329 optimizer approach for electrical parameters extraction of solar panel models. *Energy Reports*, 8, 14888-14900.
- 330 Sun, B., Li, W., Huang, Y., & Ieee. (2022). Performance of Composite PPSO on Single Objective Bound Constrained

331 Numerical Optimization Problems of CEC 2022. In *IEEE Congress on Evolutionary Computation (CEC)*.
332 Padua, ITALY: Ieee.

333 Sun, B., Sun, Y. F., Li, W., & Ieee. (2022). Multiple Topology SHADE with Tolerance-based Composite Framework
334 for CEC2022 Single Objective Bound Constrained Numerical Optimization. In *IEEE Congress on*
335 *Evolutionary Computation (CEC)*. Padua, ITALY: Ieee.

336 Valdez, F., Castillo, O., Cortes-antonio, P., & Melin, P. (2022). APPLICATIONS OF INTELLIGENT
337 OPTIMIZATION ALGORITHMS AND FUZZY LOGIC SYSTEMS IN AEROSPACE: A REVIEW. *Applied*
338 *and Computational Mathematics*, 21, 233-245.

339 Wang, X. W., Yan, Y. X., & Gu, X. S. (2019). Spot welding robot path planning using intelligent algorithm. *Journal*
340 *of Manufacturing Processes*, 42, 1-10.

341 Xiao, Y. N., Guo, Y. L., Cui, H., Wang, Y. W., Li, J., & Zhang, Y. P. (2022). IHAOAVOA: An improved hybrid
342 aquila optimizer and African vultures optimization algorithm for global optimization problems. *Mathematical*
343 *Biosciences and Engineering*, 19, 10963-11017.

344 Xu, L. W., Yu, X., & Gulliver, T. A. (2021). Intelligent Outage Probability Prediction for Mobile IoT Networks
345 Based on an IGWO-Elman Neural Network. *Ieee Transactions on Vehicular Technology*, 70, 1365-1375.

346 Yang, Y. T., Chen, H. L., Heidari, A. A., & Gandomi, A. H. (2021). Hunger games search: Visions, conception,
347 implementation, deep analysis, perspectives, and towards performance shifts. *Expert Systems with Applications*,
348 177, 34.

349 Zhang, J. L., Khayatnezhad, M., & Ghadimi, N. (2022). Optimal model evaluation of the proton-exchange
350 membrane fuel cells based on deep learning and modified African Vulture Optimization Algorithm. *Energy*
351 *Sources Part a-Recovery Utilization and Environmental Effects*, 44, 287-305.

352 Zhao, W. G., Wang, L. Y., & Zhang, Z. X. (2019). Supply-Demand-Based Optimization: A Novel Economics-
353 Inspired Algorithm for Global Optimization. *Ieee Access*, 7, 73182-73206.

354

Unimodal benchmark functions

	Function equation	Dim	Range	Optimal
F1	$f_1(x) = \sum_{i=1}^n x_i^2$	30	[-100,100]	0
F2	$f_2(x) = \sum_{i=1}^n x_i + \prod_{i=1}^n x_i $	30	[-10,10]	0
F3	$f_3(x) = \sum_{i=1}^n \left(\sum_{j=1}^i x_j \right)^2$	30	[-100,100]	0
F4	$f_4(x) = \max_i \{ x_i , 1 \leq i \leq n \}$	30	[-100,100]	0
F5	$f_5(x) = \sum_{i=1}^{n-1} \left[100(x_{i+1} - x_i^2)^2 + (x_i - 1)^2 \right]$	30	[-30,30]	0
F6	$f_6(x) = \sum_{i=1}^n ([x_i + 0.5])^2$	30	[-100,100]	0
F7	$f_7(x) = \sum_{i=1}^n i x_i^4 + \text{random}[0,1)$	30	[-1.28,1.28]	0

Multimodal benchmark functions

	Function equation	Dim	Range	Optimal
F8	$f_8(x) = \sum_{i=1}^n -x_i \sin(\sqrt{ x_i })$	30	[-500,500]	$-418.9829 \times Dim$
F9	$f_9(x) = \sum_{i=1}^n [x_i^2 - 10 \cos(2\pi x_i) + 10]$	30	[-5.12,5.12]	0
F10	$f_{10}(x) = -20 \exp\left(-0.2 \sqrt{\frac{1}{n} \sum_{i=1}^n x_i^i}\right)$ $-\exp\left(\frac{1}{n} \sum_{i=1}^n \cos(2\pi x_i)\right) + 20 + e$	30	[-32,32]	0
F11	$f_{11}(x) = \frac{1}{4000} \sum_{i=1}^n x_i^2 - \prod_{i=1}^n \cos\left(\frac{x_i}{\sqrt{i}}\right) + 1$	30	[-600,600]	0
	$f_{12}(x) = \frac{\pi}{n} 10 \sin(\pi y_1) + \sum_{i=1}^{n-1} \{(y_i - 1)^2 \times$			
F12	$\left[1 + 10 \sin^2(\pi y_{i+1}) + \sum_{i=1}^n \mu(x_i, 10, 100, 4) \right] \}$	30	[-50,50]	0

,where $y_i = 1 + \frac{x_i + 1}{4}$,

$$\mu(x_i, a, k, m) = \begin{cases} k(x_i - a)^m, & x_i > a \\ 0, & -a < x_i < a \\ k(-x_i - a)^m, & x_i < -a \end{cases}$$

$$\begin{aligned} \text{F13} \quad f_{13}(x) &= 0.1 \left\{ \sin^2(3\pi x_1) + \sum_{i=1}^n (x_i - 1)^2 [1 + \sin^2(3\pi x_i + 1)] \right. \\ &\quad \left. + (x_n - 1)^2 [1 + \sin^2(2\pi x_n)] \right\} + \sum_{i=1}^n \mu(x_i, 5, 100, 4) \end{aligned}$$

30 [-50,50] 0

Fixed-dimension multimodal benchmark functions

	Function equation	Dim	Range	Optimal
F14	$f_{14}(x) = \left(\frac{1}{500} + \sum_{j=1}^{25} \frac{1}{j + \sum_{i=1}^2 (x_i - a_{ij})^6} \right)$	30	[-65,65]	1
F15	$f_{15}(x) = \sum_{i=1}^{11} \left[a_i - \frac{x_1(b_i^2 + b_i x_2)}{b_i^2 + b_i x_3 + x_4} \right]^2$	30	[-5,5]	0.00030
F16	$f_{16}(x) = 4x_1^2 - 2.1x_i^4 + \frac{1}{3}x_1^6 + x_1x_2 - 4x_2^2 + 4x_2^4$	30	[-5,5]	-1.0316
F17	$f_{17}(x) = \left(x_2 - \frac{5.1}{4\pi^2}x_1^2 + \frac{5}{\pi}x_1 - 6 \right)^2 + 10 \left(1 - \frac{1}{8\pi} \right) \cos x_1 + 10$	30	[-5,5]	0.398
F18	$f_{18}(x) = \left[1 + (x_1 + x_2 + 1)^2 (19 - 14x_1 + 3x_1^2 - 14x_2 + 6x_1x_2 + 3x_2^2) \right] \times$ $\left[30 + (2x_1 - 3x_2)^2 \times (18 - 32x_1 + 12x_1^2 + 48x_2 - 36x_1x_2 + 27x_2^2) \right]$	30	[-2,2]	3
F19	$f_{19}(x) = -\sum_{i=1}^4 c_i \exp \left(-\sum_{j=1}^3 a_{ij} (x_i - p_{ij})^2 \right)$	30	[1,3]	-3.86
F20	$f_{20}(x) = -\sum_{i=1}^4 c_i \exp \left(-\sum_{j=1}^6 a_{ij} (x_i - p_{ij})^2 \right)$	30	[0,1]	-3.32
F21	$f_{21}(x) = -\sum_{i=1}^5 \left[(X - a_i)(X - a_i)^T + c_i \right]^{-1}$	30	[0,10]	-10.1532
F22	$f_{22}(x) = -\sum_{i=1}^7 \left[(X - a_i)(X - a_i)^T + c_i \right]^{-1}$	30	[0,10]	-10.4028
F23	$f_{23}(x) = -\sum_{i=1}^{10} \left[(X - a_i)(X - a_i)^T + c_i \right]^{-1}$	30	[0,10]	-10.5363

357 **Appendix 2**

	Function	Functions	F_i^*
Unimodal Function	F1	Shifted and full Rotated Zakharov Function	300
Basic Functions	F2	Shifted and full Rotated Rosenbrock's Function	400
	F3	Shifted and full Rotated Expanded Schaffer's f_6 Function	600
	F4	Shifted and full Rotated Non-Continuous Rastrigin's Function	800
	F5	Shifted and full Rotated Levy Function	900
Hybrid Functions	F6	Hybrid Function 1 (N = 3)	1800
	F7	Hybrid Function 2 (N = 6)	2000
	F8	Hybrid Function 3 (N = 5)	2200
Composition Functions	F9	Composition Function 1 (N = 5)	2300
	F10	Composition Function 2 (N = 4)	2400
	F11	Composition Function 3 (N = 5)	2600
	F12	Composition Function 3 (N = 6)	2700
Search range: $[-100, 100]^D$			

358